EXPERIMENTAL STUDY OF THE THERMAL-HYDRAULIC PHENOMENA IN THE REACTOR CAVITY COOLING SYSTEM AND ANALYSIS OF THE EFFECTS OF GRAPHITE DISPERSION

A Thesis

by

RODOLFO VAGHETTO

Submitted to the Office of Graduate Studies of
Texas A&M University
in partial fulfillment of the requirements for the degree of

MASTER OF SCIENCE

May 2011

Major Subject: Nuclear Engineering

Experimental Study of the Thermal-Hydraulic Phenomena

in the Reactor Cavity Cooling System and Analysis of the

Effects of Graphite Dispersion

EXPERIMENTAL STUDY OF THE THERMAL-HYDRAULIC PHENOMENA IN THE REACTOR CAVITY COOLING SYSTEM AND ANALYSIS OF THE EFFECTS OF GRAPHITE DISPERSION

A Thesis

by

RODOLFO VAGHETTO

Submitted to the Office of Graduate Studies of
Texas A&M University
in partial fulfillment of the requirements for the degree of

MASTER OF SCIENCE

Approved by:

Chair of Committee,	Yassin A. Hassan
Committee Members,	William H. Marlow
	Victor M. Ugaz
Head of Department,	Raymond J. Juzaitis

May 2011

Major Subject: Nuclear Engineering

ABSTRACT

Experimental Study of the Thermal-Hydraulic Phenomena in the Reactor Cavity Cooling System and Analysis of the Effects of Graphite Dispersion. (May 2011)

Rodolfo Vaghetto, B.En., University of Palermo, Italy

Chair of Advisory Committee: Dr. Yassin A. Hassan

An experimental activity was performed to observe and study the effects of graphite dispersion and deposition on thermal hydraulic phenomena in a Reactor Cavity Cooling System (RCCS). The small scale RCCS experimental facility (16.5cm x 16.5cm x 30.4cm) used for this activity represents half of the reactor cavity with an electrically heated vessel. Water flowing through five vertical pipes removes the heat produced in the vessel and releases it in the environment by mixing with cold water in a large tank. Particle Image Velocimetry (PIV) technique was used to study the velocity field of the air inside the cavity. A set of 52 thermocouples was installed in the facility to monitor the temperature profiles of the vessel and pipes walls and air. 10g of a fine graphite powder (particle size average 2μm) were injected into the cavity through a spraying nozzle placed at the bottom of the vessel. Temperatures and air velocity field were recorded and compared with the measurements obtained before the graphite dispersion, showing a decrease of the temperature surfaces which was related to an increase in their emissivity. The results contribute to the understanding of the RCCS capability in case of an accident scenario.

ACKNOWLEDGEMENTS

This work is part of a project that was sponsored by the US Department of Energy (DOE) and Nuclear Energy University Program (NEUP).

All the experimental activity described in this thesis was shared with Luigi Capone. The author would like to thank him for his technical advice.

Special thanks go to the advisor of the research and chair of the committee, Dr. Hassan, for his constant guidance on the experimental preparation and in the interpretation of the results.

NOMENCLATURE

$\overline{F}$	= Global View Factor
h	= Convective Heat Transfer Coefficient ($W/m^2 K$)
q”	= Heat Flux (W/m^2)
T	= Temperature (K)

Greek Symbols

Δ	= Difference
σ	= Stefan-Boltzmann Constant ($W/m^2 K^4$)

Abbreviations

a.g.	= After Graphite Dispersion
b.g.	= Before Graphite Dispersion

TABLE OF CONTENTS

Page

LIST OF FIGURES

FIGURE Page

LIST OF TABLES

1. INTRODUCTION

The main challenge of the Next Generation Nuclear Plant (NGNP) Project is to find a nuclear based technology for the production of process heat, electricity, and hydrogen. This technology must provide high-temperature process heat (up to 950°C) that can be used in several industrial applications as a convenient substitution for fossil fuel, to reduce the greenhouse gas emissions. Examples of possible integration of such new technology with industrial applications requiring high-temperature process heat are hydrogen and ammonia production or coal and natural gas conversion, iron and cement manufacturing. The Very-High Temperature Gas-Cooled Reactor (VHTR), with a nominal outlet helium temperature of 950°C, has been identified as the reactor type for the Next Generation Nuclear Plant Project. Due to the high temperatures reached in the system, some components designed for standard steam-cycles plants, have to be modified or revised to operate under such temperature conditions and new passive safety systems were considered. The Reactor Cavity Cooling System (RCCS) is one of the new safety systems designed for the next generation of nuclear power plants and it will be incorporated into proposed reactor designs for the Very High Temperature Reactor (VHTR).

This thesis follows the style of *Nuclear Engineering and Design.*

This system was conceived to guarantee the integrity of the fuel, the reactor vessel and the structures inside the reactor cavity by removing the heat from the Pressurized Reactor Vessel (PRV) during both normal operation and accident scenarios. Two different reactor cavity cooling system designs are currently under discussion. The air-based cooling system, proposed by General Atomic, (see Figure 1), is a natural convection, air-based cooling system that removes heat from the reactor cavity to protect the concrete walls of the cavity during accident conditions when either the shutdown or PCSs are inoperable.

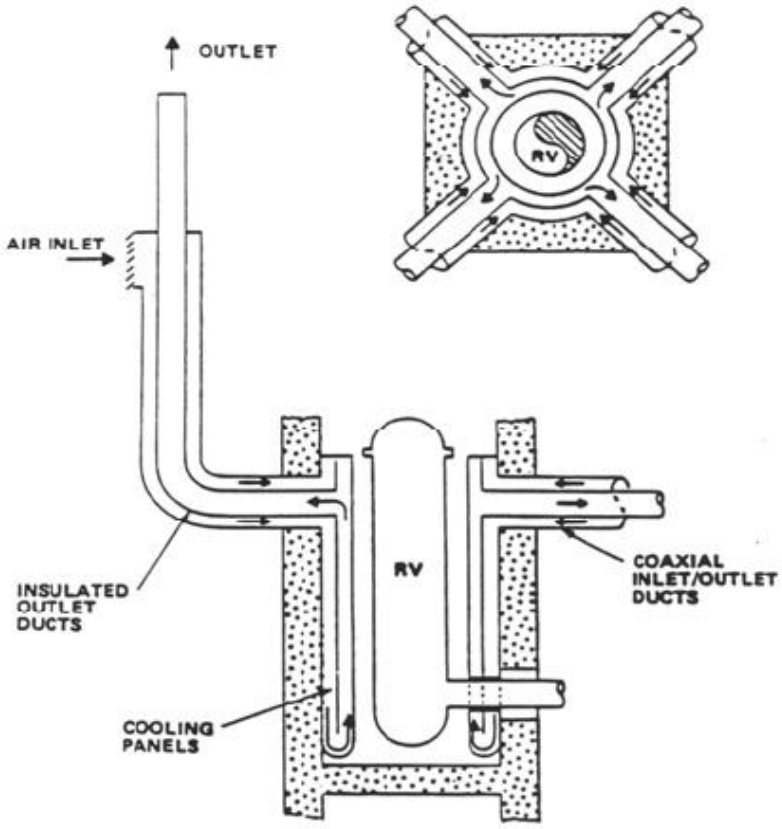

Figure 1. Air-Cooled RCCS

It is comprised of panels that line the inside of the cavity, which are connected to rising concentric ducts that lead to an outlet chimney and an air inlet. It is a completely passive design with no pumps, circulators, valves, or other active components, and is designed to operate continuously in all modes of plant operation.

The RCCS has multiple inlet/outlet ports and interconnected parallel flow paths to ensure cooling in the event of blockage of any single duct or opening, and is robustly designed to survive all credible accidents scenarios. However, even if the RCCS is assumed to fail, passive heat conduction from the core, thermal radiation from the vessel, and conduction into the silo walls and surrounding earth are sufficient to maintain peak fuel temperatures below the 1600°C design limit. The second configuration, proposed by AREVA (Figure 2), is a constant flow, water-based cooling system that removes heat from the reactor cavity to protect the concrete walls of the cavity during both normal shutdown and accident conditions. It is comprised of standpipes that line the inside of the cavity, and is a low-temperature, low pressure system with water temperatures below 30°C during normal active operation and reaching the boiling point only during emergency passive operation. In this case the RCCS can operate both in active mode by pumping water through the standpipes, or a passive mode by boiling the water for approximately 72 hour. During normal operation the heat removed from the reactor cavity by the forced convection of water is released in the atmosphere by an active secondary heat removal system. In case of accident the heat is removed by natural circulation of water and released in the atmosphere by evaporation.

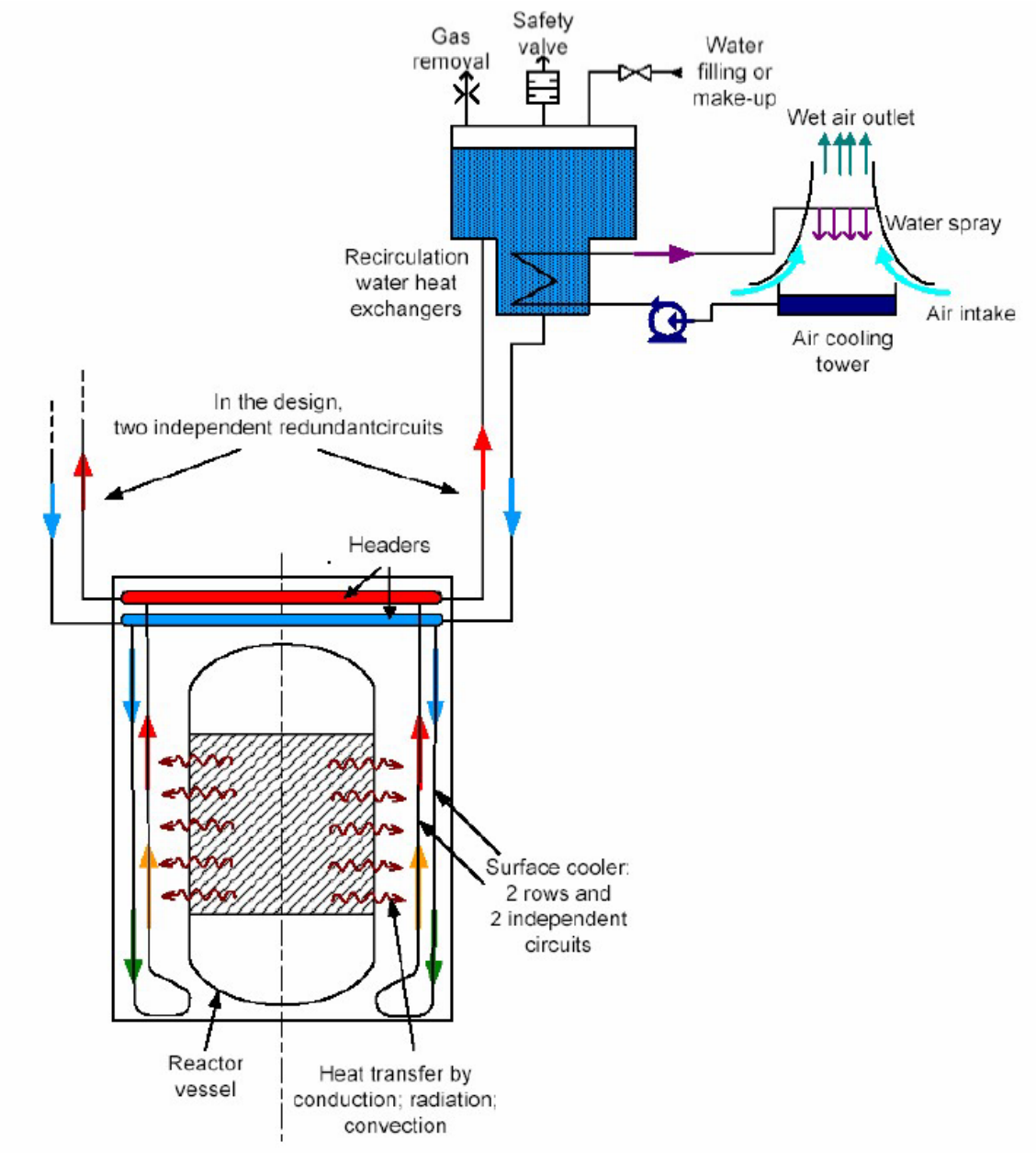

Figure 2. Water-Cooled RCCS

In both configurations, since the reactor vessel is not thermically insulated, a small portion of the heat produced in the core is released into the reactor cavity. The heat is transferred by conduction through the vessel wall and released to the RCCS coolant by convection within the air of the reactor cavity and radiation between the outer vessel surface and the riser's walls. The heat transferred to the coolant is the driving mechanism for natural circulation. Cold coolant (from the water tanks for the water-cooled configuration or from the inlet chimney in the air-cooled configuration) flows through the downcomers. The buoyancy forces produced by the difference in the density of the fluid due to the temperature gradient established by the heat transfer push the coolant to move up through the risers. The coolant coming from different risers is collected in horizontal headers or upper plena. In the air-cooled configuration the air is then discharged into the atmosphere through the outlet chimneys. In the water-cooled configuration, water reached the water tanks, mixes with cold water and comes back into the loop. As mentioned above, the RCCS is used during normal operation to keep the concrete temperature sufficiently low and during accident scenario, when the Power Conversion System (PCS) and the Shutdown Cooling System (SCS) may not be available, to maintain the temperature of concrete, vessel and core within the design limits.

The RCCS is designed to guarantee the removal of about 0.6MW, a small fraction of the thermal power generation, during normal operation and up to 1.5MW in case of accident. The thermal hydraulic behavior of the air moving into the cavity and of the coolant into the reactor cavity cooling system is quite complex due to concurrent heat transfer mechanisms such as conduction, convection and radiation. The system's heat removal effectiveness is strongly affected by different factors including geometry (risers length and dimensions, number of risers, walls thickness, total elevation change), physical properties of the materials (emissivity, thermal conductivity, heat capacitance) and thermal conditions (temperatures throughout the system). Additional factors must be taken into account in the two proposed configurations. Air-cooled systems are affected by the outside conditions such as ambient temperature or wind intensity and direction. Water-cooled configuration is mainly affected by the water inventory and initial temperature of the coolant.

1.1 Accident Scenarios of Importance in VHTR

Even though the full spectrum of accident scenarios of importance is not yet defined, the following Design Basis Accidents must be analyzed:

a. Loss of Heat Transport System and Shutdown Cooling System, also known as Pressurized Conduction Cooling (PCC) Event
b. Loss of Heat Transport System without Control Rod Trip
c. Accidental Withdrawal of a group of Control Rods followed by Reactor Shutdown
d. Unintentional Control Rod Withdrawal together with a failure of Heat Transport System and Shutdown Cooling System
e. Earthquake-initiated trip of Heat Transport System
f. LOCA event in conjunction with water ingress from failed Shutdown Cooling System
g. Large Break LOCA, also known as Depressurized Conduction Cooling (DCC) Event
h. Small Break LOCA

All the accident scenarios releasing coolant into the cavity (f, g and h in the list above) are of particular interest for this research project since they may affect the thermal hydraulic phenomena in the Reactor Cavity Cooling Systems. Among those, the DCC event is considered the most demanding and most likely to lead to higher vessel and fuel temperatures. The DCC scenario starts from a full reactor power condition and

is initiated by a double-ended guillotine break of both cold and hot ducts. The depressurization transient is expected to be very rapid and, even if the reactor trips immediately to decrease the core power down to the decay heat level, the core is expected to heat up due to the decrease in the heat removal. This is mainly caused by the loss of forced convection of the coolant and the system depressurization. In particular, during blowdown, the graphite dust produced and accumulated in the reactor system is transported into the reactor cavity and the heat transfer mechanisms, such as radiation, which was found to be of paramount importance by Van Antwerpen et al. (2008), and convection may be affected. The phenomena following this phase of the accident, studied in details by Loyalka (1983), are not object of this research project but are described for completeness. Once the system depressurization is complete (pressures of reactor system and cavity equalize), the system power level, the heat transfer from the fuel to the core, to the vessel and, finally to the environment via the RCCS are the only controlling boundary conditions that govern the system temperature. Temperature of the fuel increases while air from the cavity enters into the reactor vessel by molecular diffusion. This increase continues until the core heat production is balanced by the heat removal operated by the RCCS. Later, the extensive graphite oxidation due to the increased concentration of air produces a large amount of heat which causes a second peak in the core temperature. When air is depleted graphite oxidation stops and the fuel temperature starts to decrease again. A core safe shutdown state is eventually reached.

1.2 Project Technical Objective

Kissane et al. (2010), studying the behavior of graphite dust in High Temperature Reactors (HTR), predicted a relatively large amount of carbonaceous dust produced during the operation of such systems. This amount, considerably greater in pebble bed than prismatic systems, was estimated to be as much as 100kg/yr for a 400MWt unit. As stated in the previous section, in the case of a loss of coolant accident, such as Depressurized Conduction Cooling (DCC) event, graphite dust can be resuspended into the coolant and eventually discharged into the reactor cavity and deposited on the cavity surfaces. The main purpose of this project is to evaluate the effects of graphite dispersion and deposition into the reactor cavity of a VHTR following a loss of coolant accident. In particular, this study quantitatively and qualitatively evaluates any possible impact on the radiation heat transfer mechanism and the phenomena associated with the natural circulation of air inside the cavity. The experimental activity was carried out using the Texas A&M RCCS Experimental Facility located in the thermal hydraulic laboratory located in the Department of Nuclear Engineering. The experimental apparatus will be presented and described in details in the next sections. It has to be mentioned that experimental data such as walls temperature profiles, inlet/outlet coolant temperatures, air temperature profile velocity map were collected and used to validate computer code predictions such as CFD and RELAP5-3D. Comparisons are not part of the objective of this thesis and will not be presented.

2. EXPERIMENTAL FACILITY OVERVIEW

The Texas A&M experimental facility is a small scale test facility conceived to observe and study heat transfer phenomena occurring in the Reactor Cavity Cooling System (Capone at al., 2010b).The model represents half of the reactor cavity with the reactor vessel at the center and five vertical pipes for reactor cooling. An overview of the test facility with the actual layout of the components is presented in Figure 3.

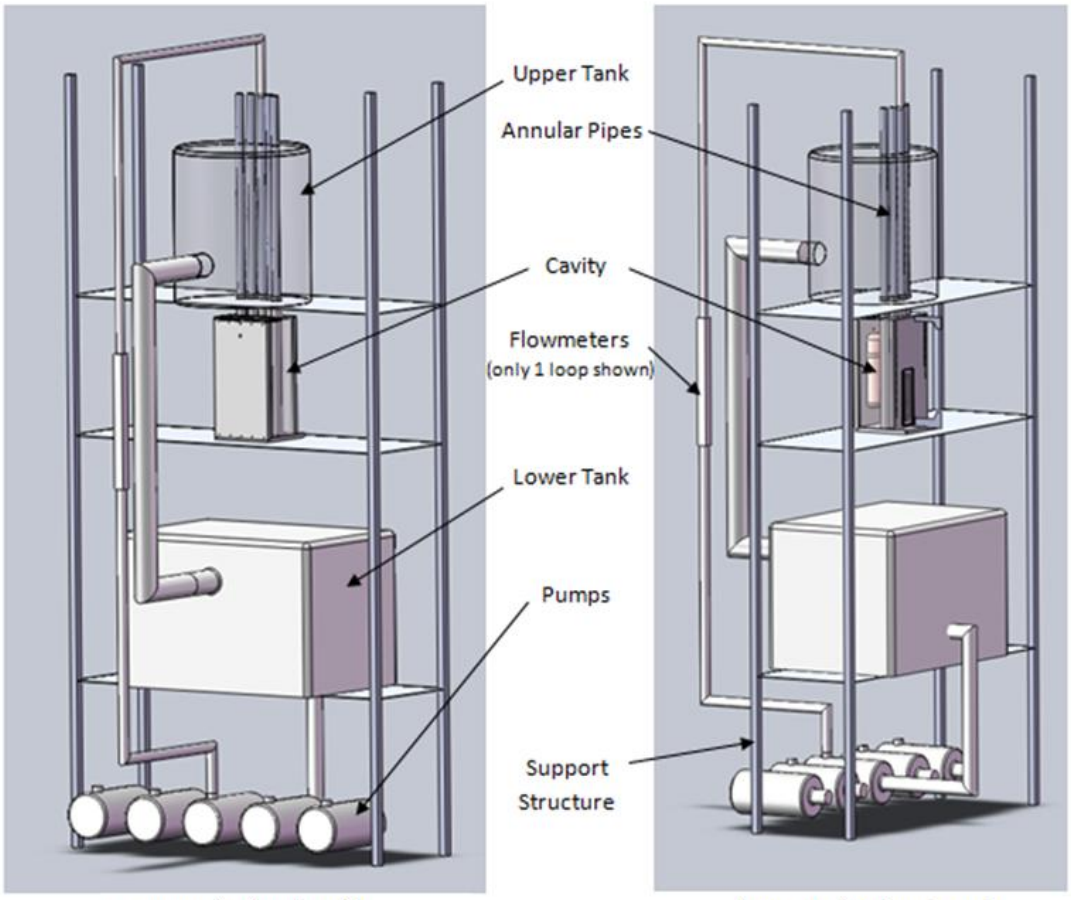

Figure 3. Experimental Facility Overview

The main components of the facility are the reactor vessel, the standing pipes, the reactor cavity, the top and bottom tanks and the pumps. The reactor vessel is a copper semi-cylinder fixed on the front wall of the cavity, heated by two electrical heater rods inserted into two parallel cylindrical holes from the top of the vessel (Figure 4). Five stainless steel vertical annular pipes are positioned in front of the vessel along a circumference arc inside the reactor cavity as shown in Figure 5.

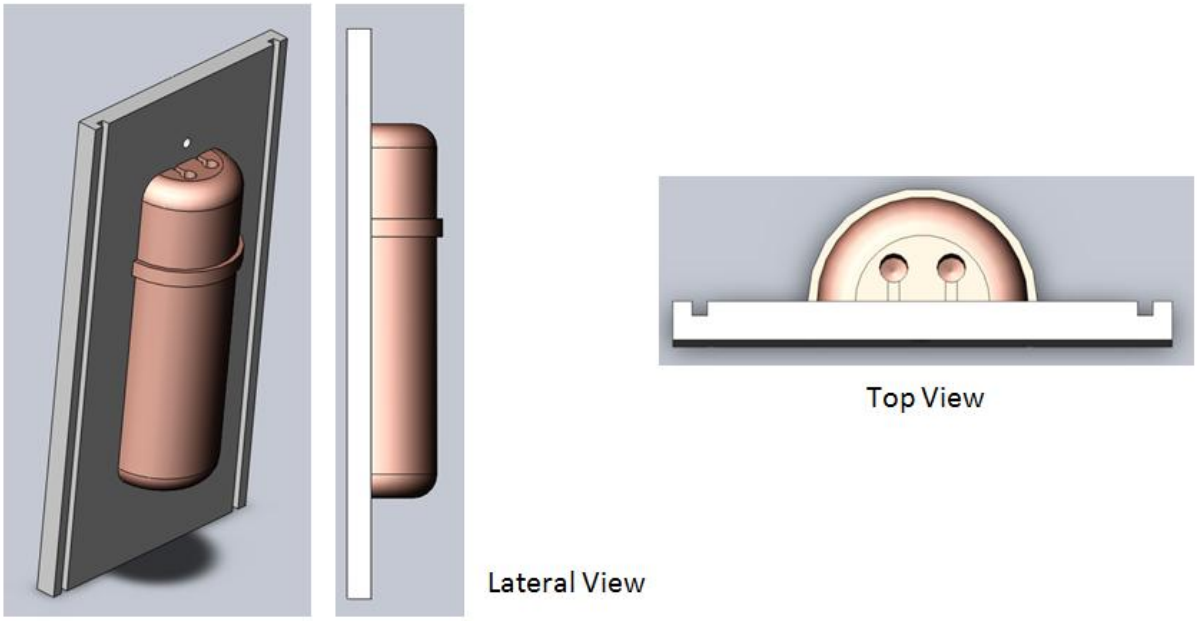

Figure 4. Reactor Vessel

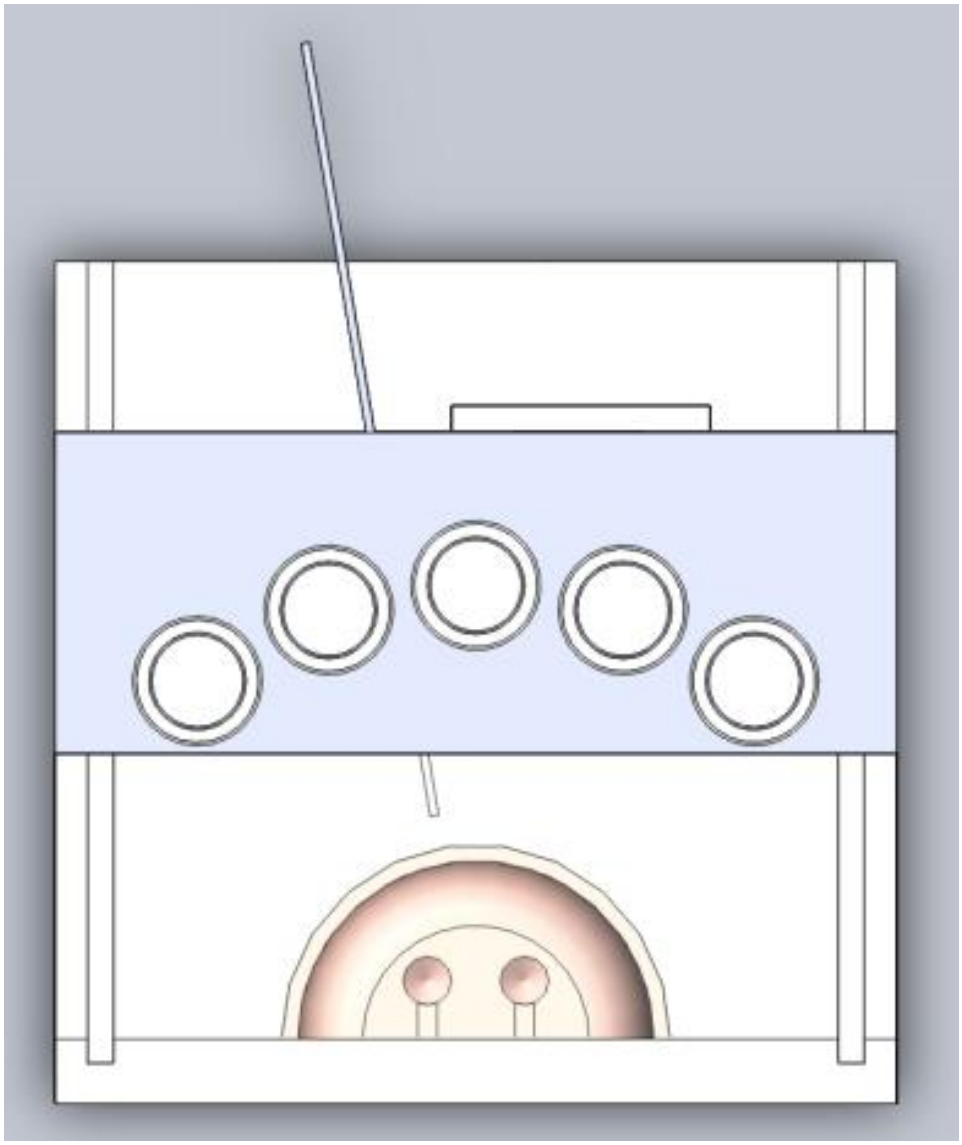

Figure 5. Cavity Top View

The flow path over the experimental facility is depicted in Figure 6. Cold water from the bottom tank is pumped into the inner section of the five standing pipes through the lid of the top tank. The water goes down through the pipes and reaches the cavity lower plenum where the flow is directed to the annular section. While moving up toward the upper tank, the water removes the heat produced in the vessel. The coolant now leaves the pipe right at the entrance of the upper tank gravity moves it toward the lower tank. Hot water mixes with the cold water in the lower tank and a new cycle starts. Appendix A contains additional pictures of the experimental facility.

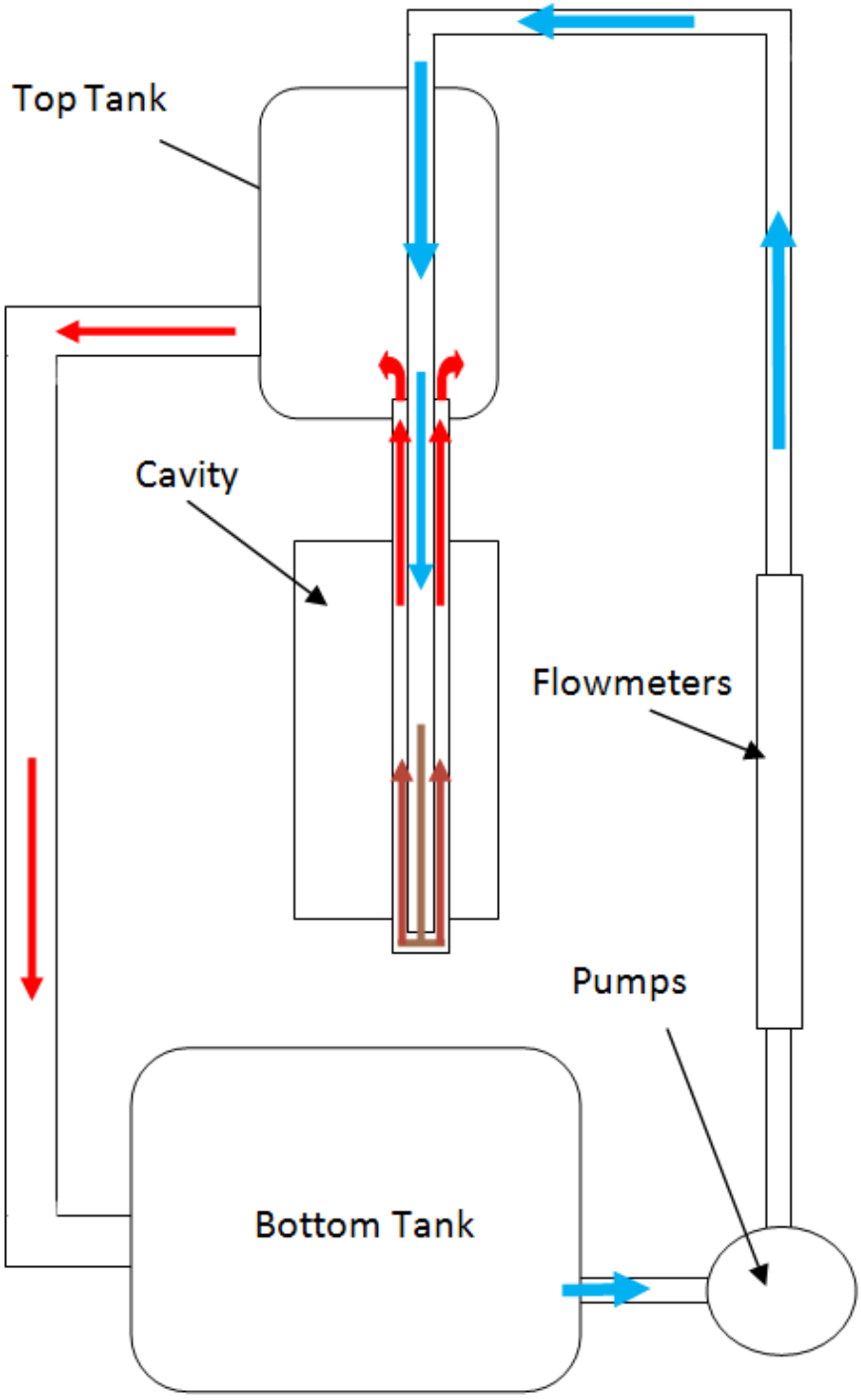

Figure 6. Coolant Flow Path

3. INSTRUMENTATION

The facility described above is equipped with several types of instrumentation in order to measure the thermodynamic quantities of interest such as walls, air and water temperatures, mass flow rates, and electric power. Lateral walls of the cavity are made of Pyrex in order to carry out any kind of visualization inside the cavity. The facility was coupled with a laser and camera, set to evaluate the velocity of air inside the cavity using Particle Imaging Velocimetry (PIV) which will be described in the next subsections.

3.1. Thermocouples

All the thermocouples used in the Texas A&M RCCS Test Facility were K-Type thermocouples. This type of thermocouples is characterized by a good sensitivity, a low cost and a wide variety of probes. The temperature profile of the outer surface of the vessel was measured with 18 thermocouples placed along the vertical midline as shown in Figure 7. Thermocouples were tightened to the surface with screws and electrically connected to the external instrumentation via insulated electrical wires running along the surface of the vessel.

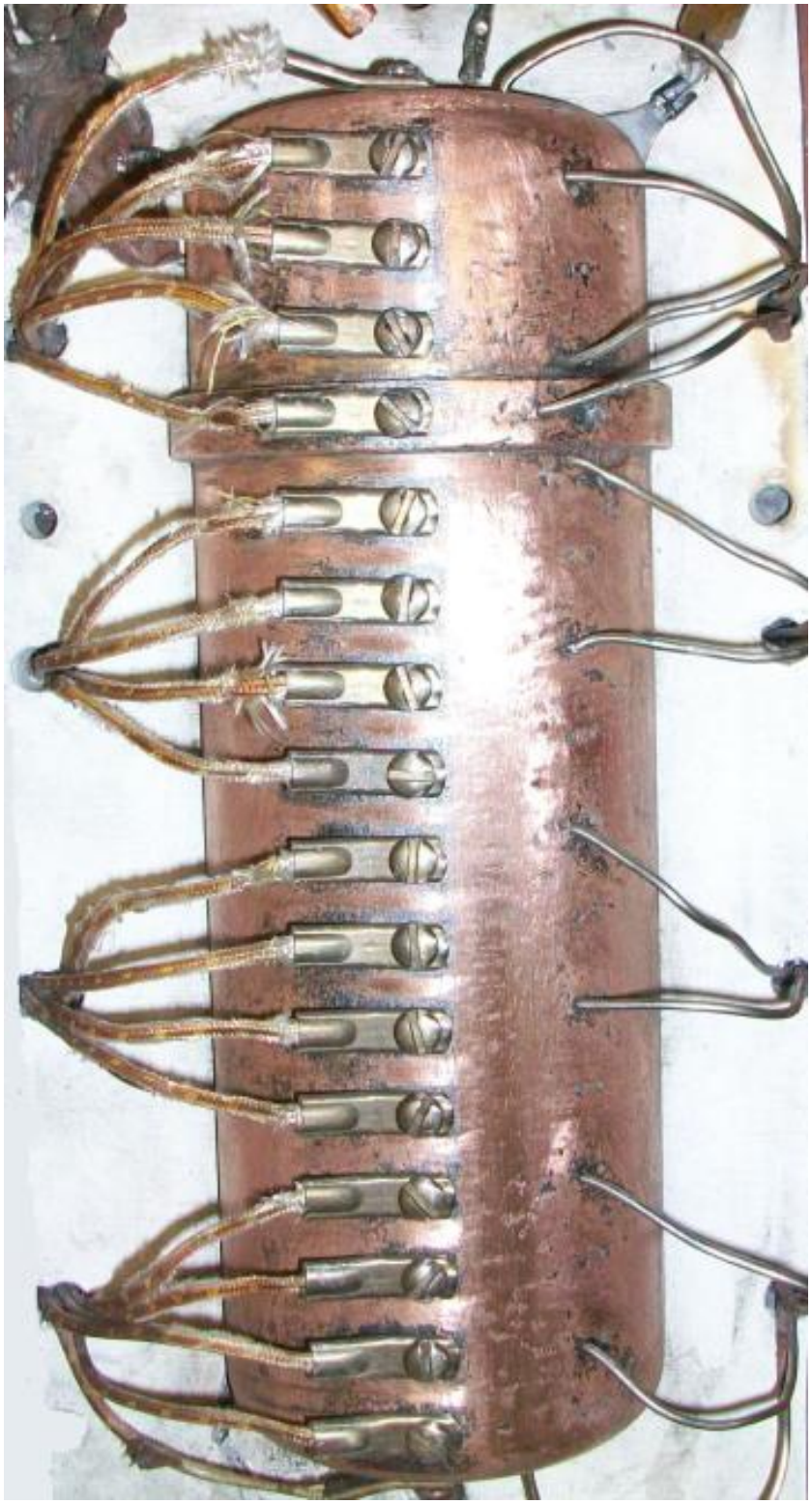

Figure 7. Vessel Thermocouples Placement

Eight thermocouples of the same type used on the vessel were mounted along the external surface of the central vertical pipe to measure the pipe wall temperature profile. The thermocouples were welded on the external pipe surface. High thermal conductivity glue was also applied in order to improve the thermal contact between the pipe surface and the tip of each thermocouple and reduce errors in the measurement. Electrical wires, in this case, ran between the adjacent pipes to the back of the cavity and electrically connected to the data acquisition system. Also in this case the thermocouples cable is thermically and electrically insulated. The insulation was removed only at both ends to allow the electrical connection and the welding. Figure 8 presents a picture of the 5 vertical pipes taken from the inside of the cavity, showing how the thermocouples are placed. The pitch between the welding points was set to around 3.5 centimeters. The distance between the first thermocouple and the bottom of the cavity was set to approximately 1 centimeter.

Figure 8. Riser Thermocouples Placement

Two additional probes were placed inside the upper and lower tanks. The one placed inside the upper tank was conceived to monitor the outer coolant temperature. The inner temperature of the water was monitored using the thermocouple placed at the entrance of the 5 exit pipelines inside the bottom cavity (Figure 9).

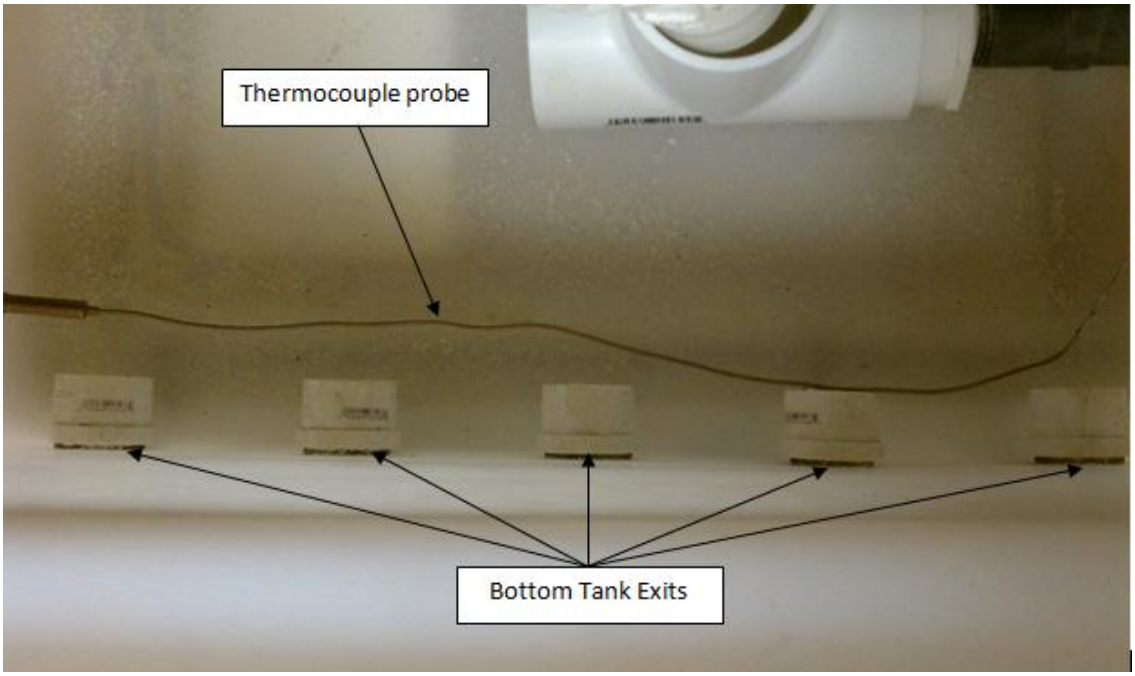

Figure 9. Thermocouple inside the Bottom Tank

The temperature profile of the air inside the cavity was produced by a set of 24 thermocouples mounted on a movable rack. The rack could be placed a different radial locations in the cavity between the vessel and the pipes and could be moved during the operation of the facility without removing any insulation panel. This structure was conceived to monitor the temperatures of the air at different positions from the vessel surface (Figure 10). Two additional thermocouples (not shown in Figure 10) were placed

at the inner and outer surface of the back panel to estimate the heat loss through the back wall of the cavity.

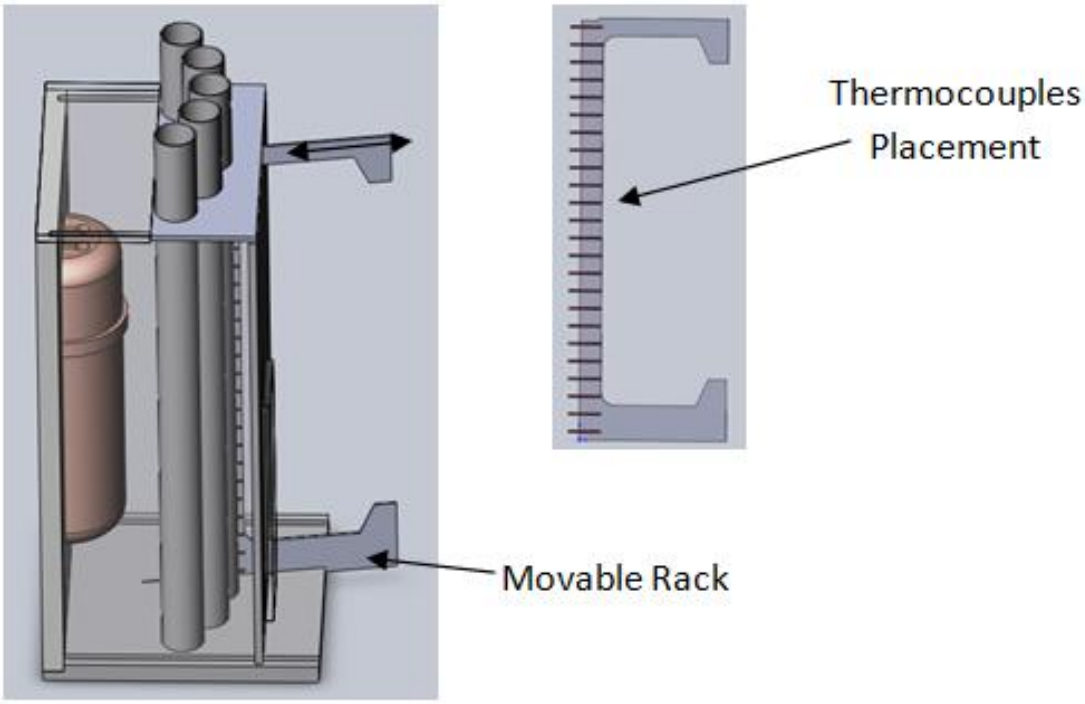

Figure 10. Cavity Rack and Thermocouples

3.2. Temperature Data Collection System

All the thermocouples above mentioned are connected to a dedicated external device set for data recoding and processing. The set is made of three main components (Figure 11):

- AC Powered Chassis
- Thermocouple Terminal Blocks
- Personal Computer

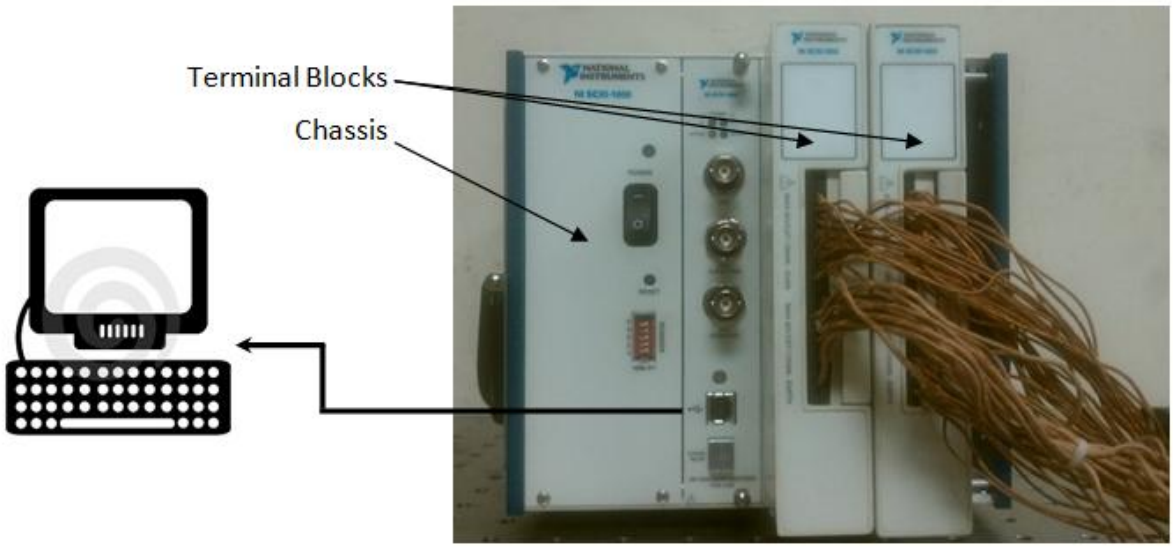

Figure 11. Temperature Data Acquisition System

The SCXI™ 1000 National Instruments™ chassis is an AC powered case which is able to house up to three thermocouple terminal blocks, providing a low noise environment and high speed signal multiplexing. Its compatibility with Windows XP® operative system makes the system easy-to-connect to a personal computer via USB port located on the front panel. Two SCXI™ 1300 National Instruments™ terminal blocks were connected to the chassis to collect and process the signals coming from the thermocouples installed inside the facility. Table 1 lists the major characteristics of the data collection system.

Table 1. Temperature Data Collection System Specifications

Accuracy	1.3 °C
Repeatability	0.5 °C
Sensor Output	±10mV/°C

3.3. Flowmeters

The mass flow rate of water through each of the five vertical pipelines was controlled independently setting a different opening of the valves positioned at the exit of each pump. Mass flow rates were monitored using analog flowmeters placed downstream of the mentioned valves. The operative range of the flowmeters is 0.5 to 5 gpm. A picture of the flow meters used and their location is shown on Figure 12.

Figure 12. Mass Flow Rate Measurement and Control

3.4. Electrical Power System

As mentioned above, two electrical heaters were placed into the vessel to produce the heat required for the experiments. The heaters were powered by an analog transformer with an adjustable output voltage within zero and 100% of the maximum allowable voltage (140V). The transformer was coupled with a power meter to measure the electric power supplied to the heaters and, subsequently, the total thermal power produced in the vessel. Figure 13 shows the electrical scheme used for electrical power measurements.

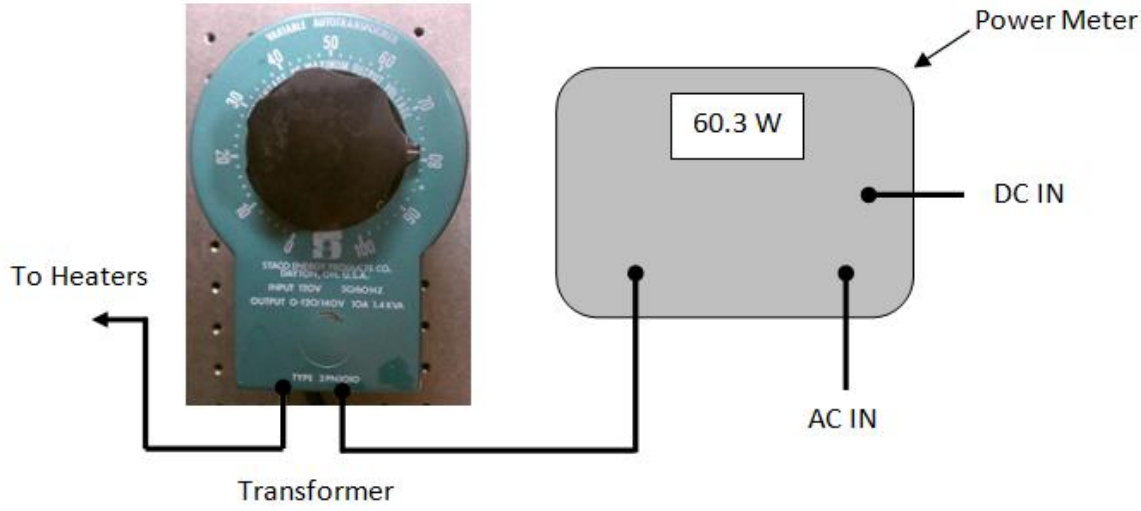

Figure 13. Power Supply System

3.5. Particle Image Velocimetry (PIV) Apparatus

The scheme presented in Figure 14 shows the main components of the particle image velocimetry apparatus used to estimate the velocity of the air in the cavity.

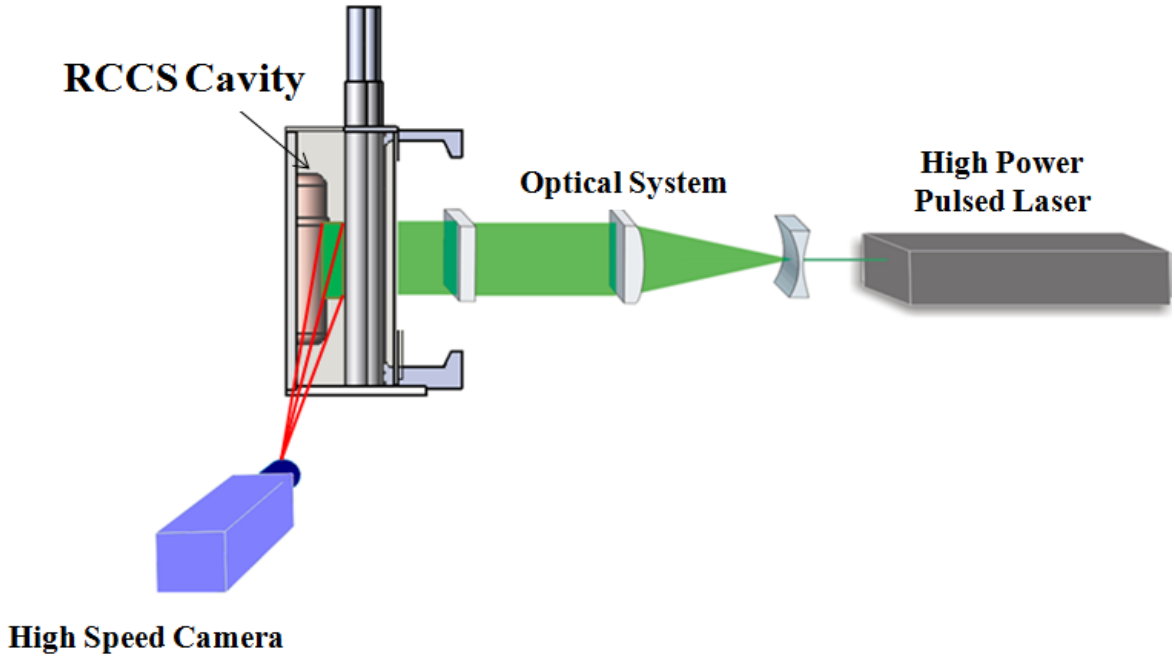

Figure 14. PIV Apparatus (Capone et al. 2010a)

The apparatus contains:

- High Power Pulsed Laser
- Optical System (Lenses)
- High Speed Camera

A high speed laser (ESI® New Wave Research, Pegasus PIV, wavelength of 527 nm, maximum energy of 10 mJ per pulse) provided illumination for the PIV analysis. Pegasus PIV is a compact, high speed, dual laser-head system designed to provide a highly stable green light source for Particle Image Velocimetry (PIV) applications. An optical fiber was used to transport the laser beam from the laser head system to the location of the experimental facility. To produce a vertical laser sheet of desired thickness (1 mm), the illumination source was properly manipulated through a set of two cylindrical lenses and pointed toward the opening window positioned in the midplane of the back wall of the cavity. The laser head was coupled and synchronized with a high speed/high resolution camera (Vision Research, Phantom v7.3, 800 _ 600 pixels, 12 bit) to capture images of the illuminated section of the cavity at a rate of 1000 frames per second (fps). A motor-driven slide system (Velmex BiSlide®) was installed to perform axial course adjustment and/or fine alignment of the camera and the fiber optic/lenses system during the experiment, in order to achieve the best illumination throughout the length of the cavity. It must be remarked that this apparatus has been already successfully used for analysis water flow by Estrada-Perez et al.(2010). PIV technique was already described in details by Hassan et al. (1992).

3.6. Particle Sizer Spectrometer

The size of the particles of graphite and tracking material used during the experiments was evaluated with the TSI ™ Aerodynamic Particle Sizer ® Spectrometer (Figure 15). The APS sizes particles in the range from 0.5 to 20 micrometers using a sophisticated time-of-flight technique that measures aerodynamic diameter in real time.

Figure 15. Particle Sizer Spectrometer (www.tsi.com)

The APS accelerates the aerosol sample flow through an accelerating orifice. The aerodynamic size of a particle determines its rate of acceleration, with larger particles accelerating more slowly due to increased inertia. As particles exit the nozzle, they cross

through two partially overlapping laser beams in the detection area. Light is scattered as each particle crosses through the overlapping beams. An elliptical mirror, placed at 90 degrees to the laser beam axis, collects the light and focuses it onto an avalanche photodetector (APD). The APD then converts the light pulses into electrical pulses. The use of two partially overlapping laser beams results in each particle generating a single two-crested signal. The scheme described above is presented in Figure 16.

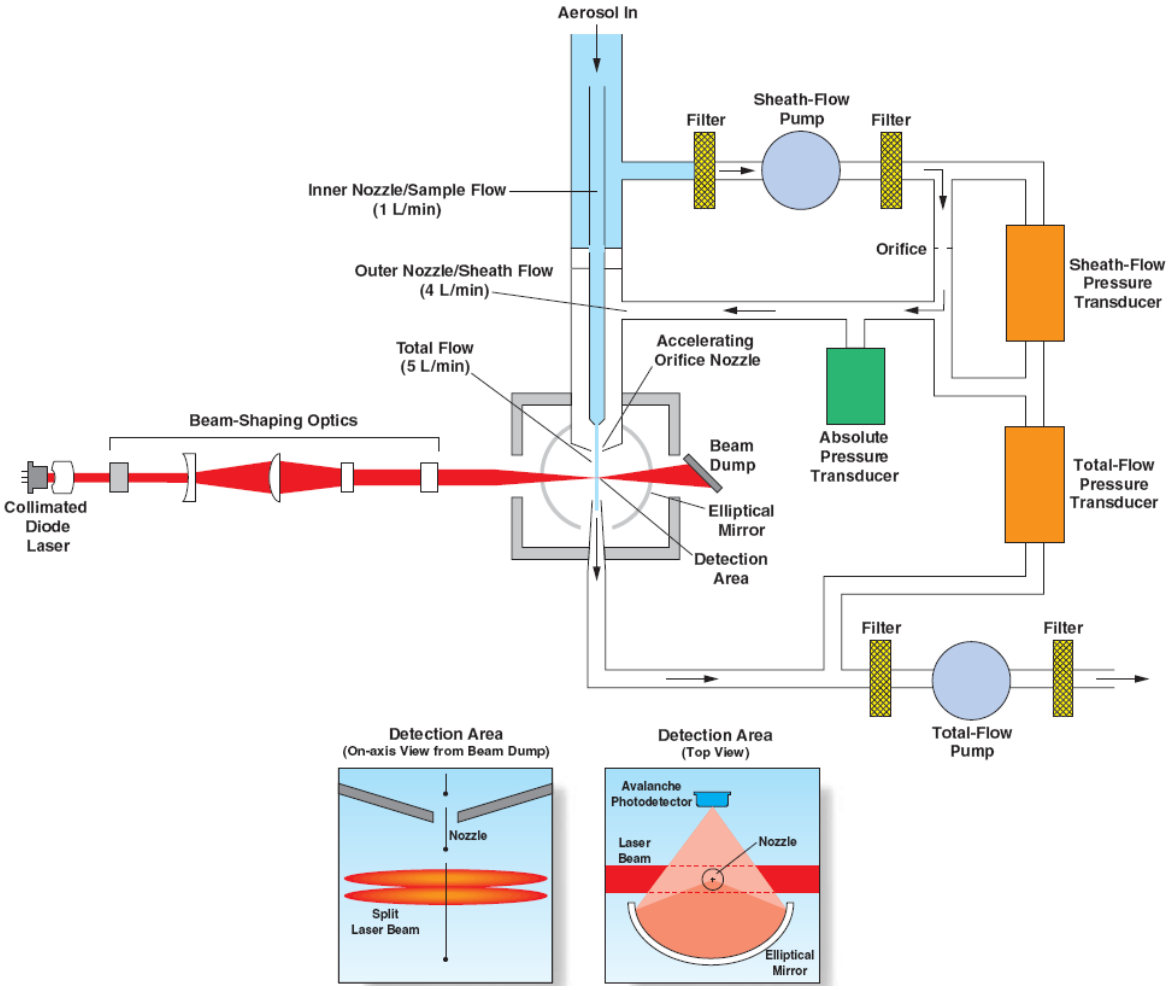

Figure 16. Sizer Internal Scheme (www.tsi.com)

Peak-to-peak time-of-flight is measured with 4-nanosecond resolution for aerodynamic sizing. The amplitude of the signal is logged for light-scattering intensity. The smallest particles may have only one detectable crest and are binned separately. In uncorrelated mode, these particles are displayed in the smallest size channel (less than 0.523 micrometer). Particles with more than two crests, indicative of coincidence, are also binned separately but are not used to build aerodynamic-size or light-scattering distributions. The particle sizer was coupled with a personal computer for data acquisition and processing. Table 2 summarizes the main technical characteristic of the APS.

Table 2. Sizer Characteristics (www.tsi.com)

Range	0.5 ÷ 20 µm
Resolution	0.02µm @ 1.0µm 0.03µm @ 10µm
Max Particle Concentration	10000 particles/cm^3
Min Particle Concentration	0.001 particles/cm^3

4. EXPERIMENT PREPARATION AND PROCEDURE

4.1. Particles Selection and Characterization

As previously mentioned, PIV technique was used to study the natural circulation of the air inside the cavity. Different particle tracking materials were considered for the PIV technique to study the natural circulation of the air inside the cavity. Zinc Stereate $Zn(C_{18}O_{35}H_2)_2$ was selected among a list of materials available as tracking particles due to its physical properties such as:

- ✓ Small diameter, to achieve the mechanical equilibrium with the air flow in a short time.
- ✓ Relatively Low density (0.28 g/cm^3) allowing enough time for measurements before complete sedimentation;
- ✓ White color allowing a good contrast with the dark background during camera acquisition;
- ✓ High evaporation point, to avoid particles loss due to evaporation when in contact with hot surfaces (vessel);

For a more accurate value of the particle size than the range specified in the material's datasheet, a particle size characterization was performed. The characterization was repeated at different particle concentrations in order to study the sensitivity of the instrumentation. For each concentration, three consecutive measurements were

performed and the average was calculated. Figure 17 shows the characterization of the PIV particle seed.

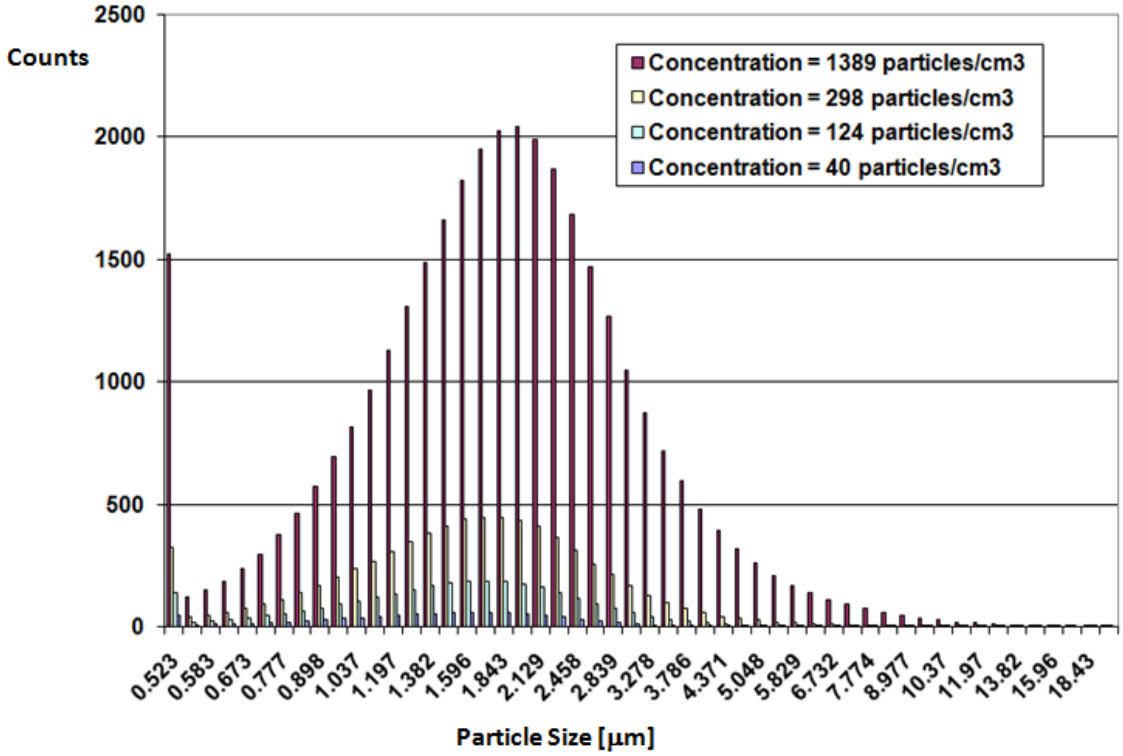

Figure 17. PIV Tracking Particles Size Characterization

The mean value of the particle size was approximately 2.2µm, with a distribution ranging between 0.5µm and 13µm. The high count at the left side of the plot is due to the contribution of all the particles with a diameter smaller than 0.523µm (instrumentation lower detectible limit).

The same approach was applied for selecting the graphite powder used to conduct the experimental analysis of the effect of graphite deposition on the cavity

surfaces. The characterization results are shown in Figure 18. In this case particular attention was dedicated to the selection based on the particle size in order to get closer to the real accident scenario.

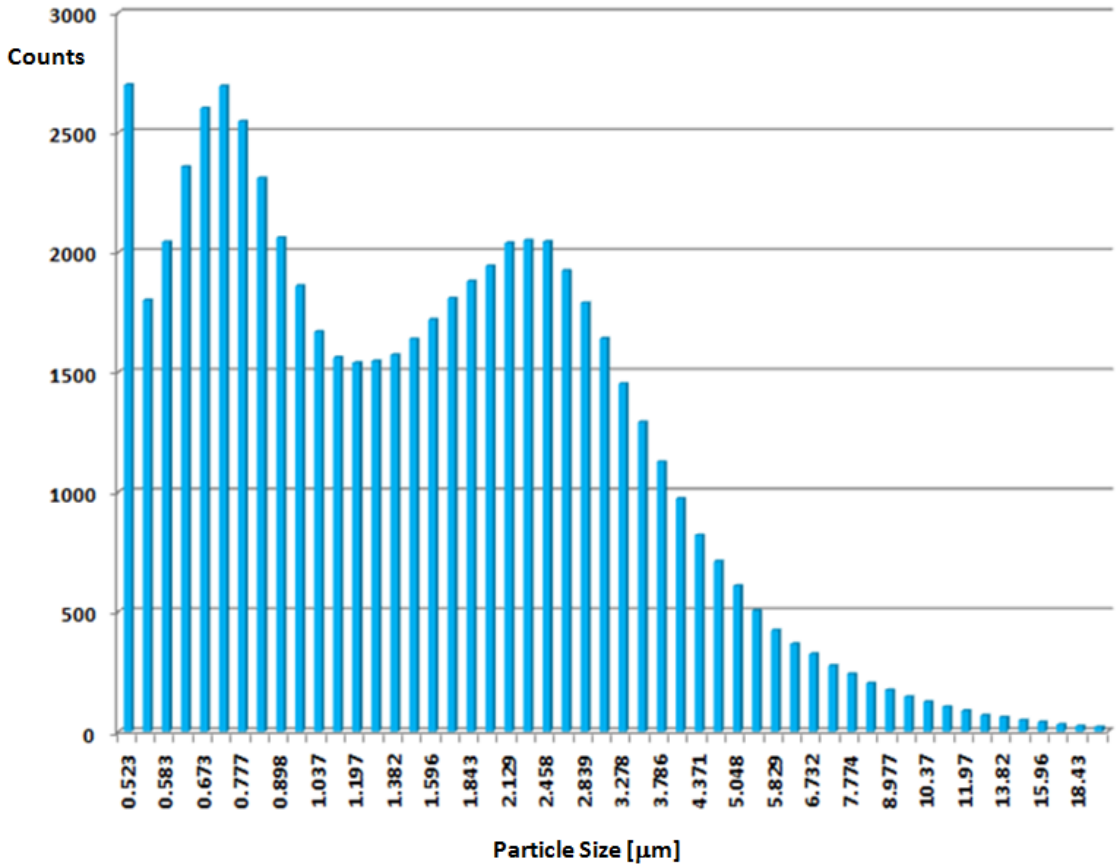

Figure 18. Graphite Particles Size Characterization

The mean size of the graphite particles was approximately 2µm (median = 1.51µm). This values aligns with the expected size of graphite dust in High Temperature Reactors (<10µm).

Pictures of the two different particles used during the experiment are shown in Figure 19 (right: PIV Particle seed, left: graphite dust)

Figure 19. Powders Used in the Experiment (left: PIV Particles; right: Graphite Dust)

4.2. Particles Injection Method

The graphite powder was dispersed by directly spraying it into the chamber through a small hole positioned right below the reactor vessel. Two different injection locations were used, instead, for the tracking particles in order to achieve the optimum seed concentration in the area of visualization (top or bottom). Compressed air was injected into a spraying gun to achieve a uniform particle distribution in the cavity in the shortest time. Figure 20 shows the RCCS scheme, the position of the injection hole and the spraying system used for the experiment.

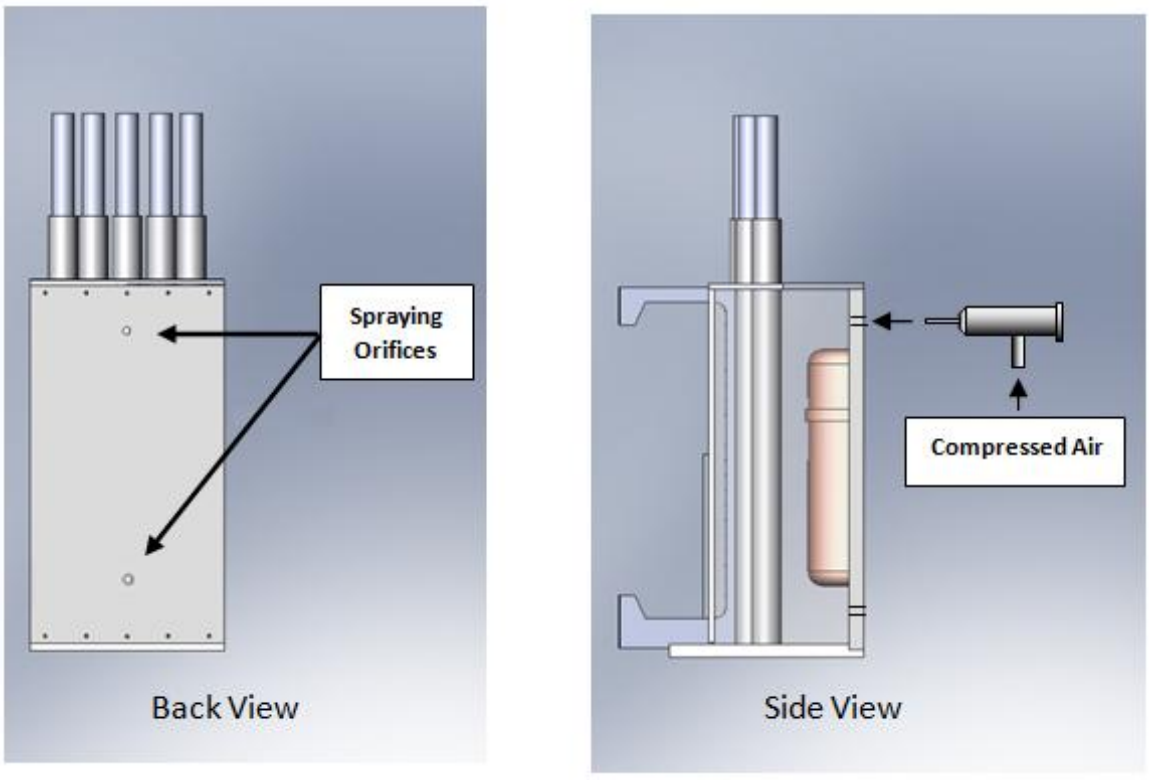

Figure 20. Particles Injection Sites and Spraying System

4.3. Experimental Procedure

Two sets of experimental measurements, with and without graphite, were carried out in order to study the effect of the graphite dispersion and deposition into the cavity. At the beginning of each experimental set, all internal surfaces of the cavity (vessel, standing pipes, and cavity walls) were properly cleaned to remove any seed residual from previous experiments. The experimental data obtained during each set was recorded only when the steady-state was achieved. Walls and air temperatures were monitored with a sampling frequency of four measurements per hour until the change in temperature between two consecutive samples was lower than the temperature acquisition system accuracy (±1.3°C). At this time steady-state was assumed to be achieved. To account for measurement fluctuations, the average of 10 consecutive acquisitions of the system temperatures was used in the final calculations. Pictures of the vessel and pipes surfaces were also taken before and after the graphite dispersion (see Appendix A). The first set of measurements was performed without graphite dust. After collecting the temperature data, the PIV analysis was started. To achieve the best illumination throughout the length of the cavity, the cavity was divided into four axial regions and the PIV acquisition was repeated for each region (Figure 21).

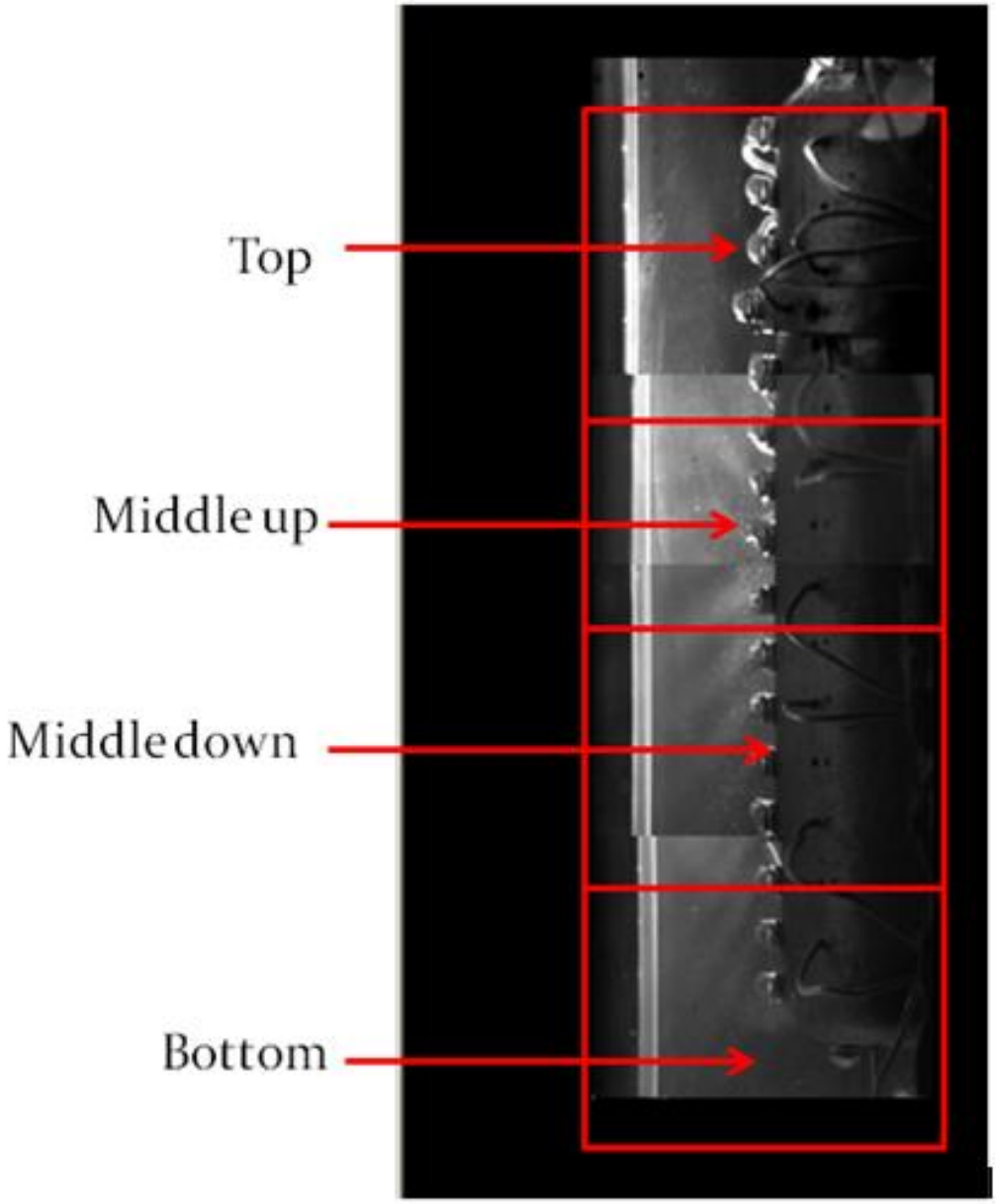

Figure 21. Cavity Axial Regions

The camera and lens system were simultaneously moved and aligned to the portion of the cavity under visualization. A small amount of seed particles was injected through one of the two injection orifices (top orifice for top and middle-top positions and bottom orifice for middle-bottom and bottom positions). A five second image acquisition was started after a uniform motion of the particles was visibly achieved. In the second set of experiments, 10 grams of graphite dust was injected into the cavity and, using the same method described above, a new set of measurements was performed only after new steady-state conditions were confirmed. It must be noted that all cavity walls were thermically insulated during the experiment to minimize the thermal losses. The thermal insulation panel of one of the lateral walls of the cavity was temporarily removed only during the camera acquisition and placed between each acquisition step. Perturbations induced by the insulation panel removal were neglected due to the short time required for the procedure (~10 s from particle injection to end of image acquisition for each axial region). The total electric power supplied to the heaters was 165W. The mass flow rate selected for each of the five loops was 0.063kg/s.

5. RESULTS AND COMMENTS

In this section the results obtained during the experimental activity are presented and commented. Temperature profiles and PIV flow visualization are organized in two different subsections. A brief description of the physical phenomena and the theory applied for the interpretation of the experimental results will be also provided.

5.1. Temperature Profiles

The vessel and pipes temperature profiles were analyzed to study the effect of the graphite dispersion. The temperature profiles of the vessel surface before and after the graphite dispersion (red and blue lines respectively) are plotted in Figure 22. The plot shows only the stationary state temperatures for each case before and after graphite dispersion.

The temperature profile of the coolant riser wall outer surface is plotted in Figure 23 for the same two cases. Also in this last the plot shows the temperatures established when the steady state was achieved.

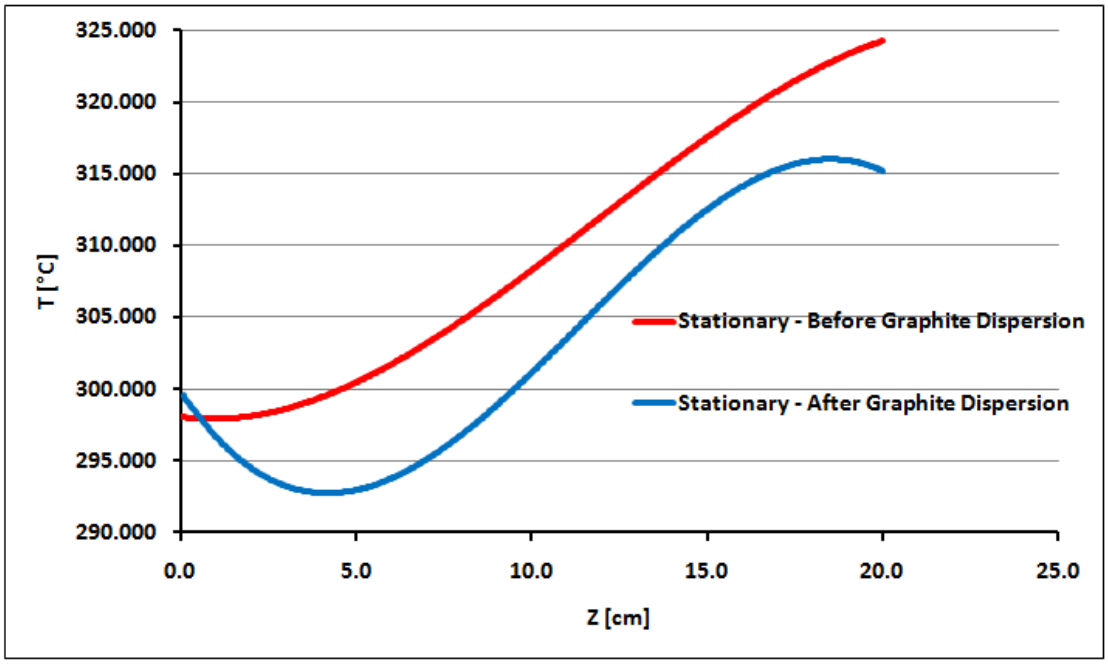

Figure 22. Vessel Surface Temperature Profile

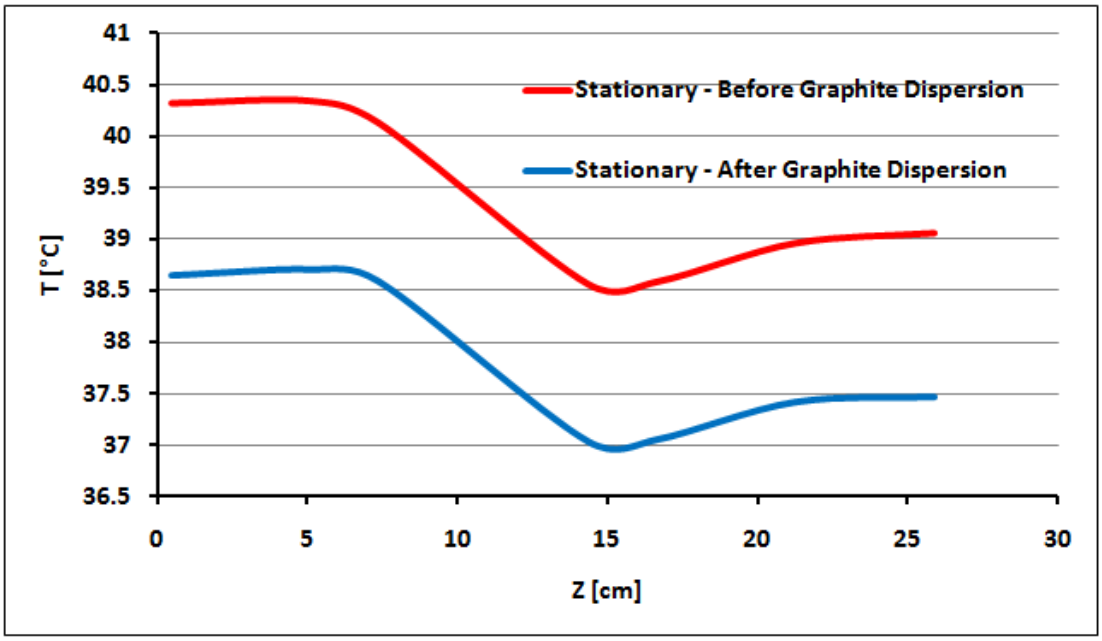

Figure 23. Outer Surface Riser Wall Temperature Profile

The effect of graphite dispersion into the cavity on the temperature profiles of the vessel and pipes surfaces was a decrease in the average temperature of both surfaces as summarized in Table 3.

Table 3. Average Temperature Summary (°C)

	Before Graphite Dispersion	After Graphite Dispersion
Vessel	308	303
Pipe	40	39

As mentioned in the previous sections, the inlet and outlet temperature of water were also measured during the experiment. Figure 24 shows these measurements before and after the graphite injection. As expected, since the total energy produced in the vessel and the total coolant mass flow rate were kept constant throughout the experiment, no effect due to the graphite dispersion was observed in the variation of the coolant temperature between the inlet and outlet of the cavity. The temperature of the air inside the cavity was also recorded at different positions of the Rack. As a reference, the temperature profile of the air recorded when the rack was moved to its closest position to the vessel is presented in Figure 25. No appreciable change in the temperature was observed after graphite dispersion.

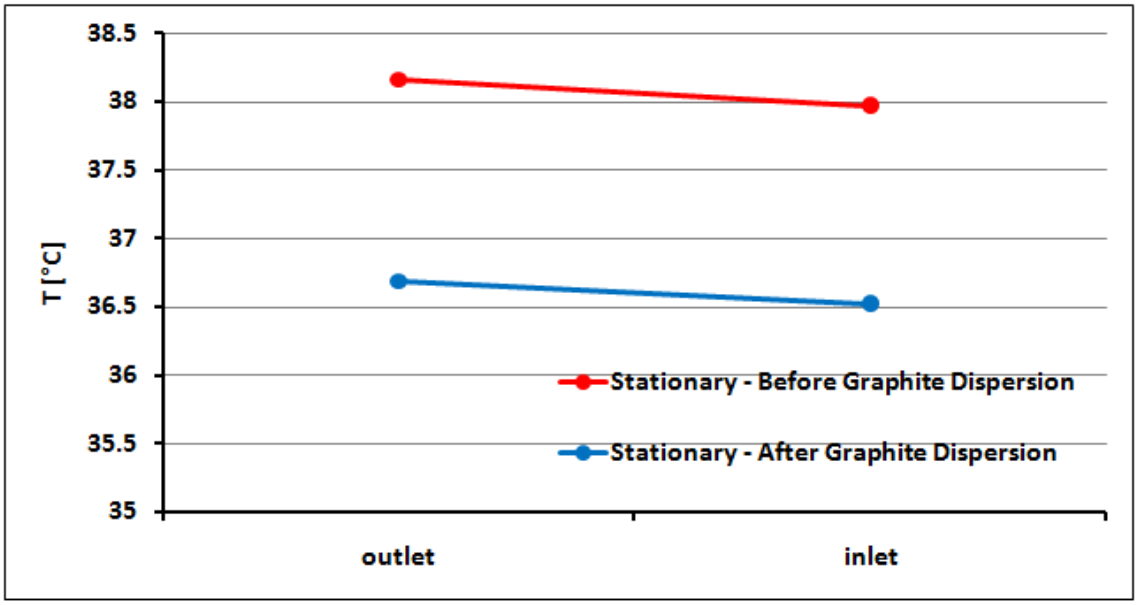

Figure 24. Inlet and Outlet Coolant Temperatures

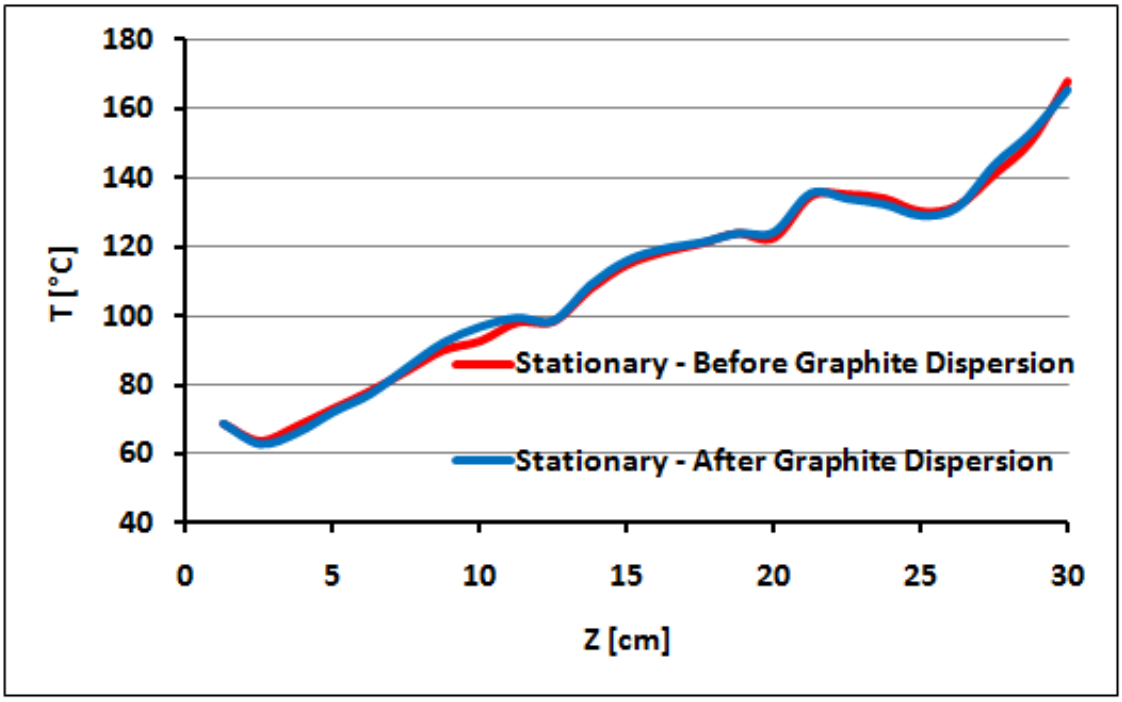

Figure 25. Air Temperature Profile

One of the most interesting behaviors that can be observed from the air temperature profile is the high temperature at the top of the cavity which is caused by the air recirculation that will be discussed in the next section. This phenomenon, combined with the high velocity field that was observed during the PIV analysis also described in the next section, is responsible for a high temperature at the ceiling of the cavity (hot spot) right above the reactor vessel. This hot spot was already predicted by the Computational Fluid Dynamic (CDF) simulations. A similar profile was observed at different locations of the rack inside the cavity as shown in Appendix B. The temperature of the air, as expected, was observed to increase along the cavity (from the bottom to the top). This behavior is mainly due to the recirculation of the air at the top of the cavity and it becomes less important near the risers where the effect of the vortex at the top of the cavity becomes less important and the cooling effect of the risers is predominant.

5.2. PIV Cavity Air Flow Visualization

A qualitative overview of the velocity field of the air inside the cavity before and after graphite injection is shown in Figure 26.

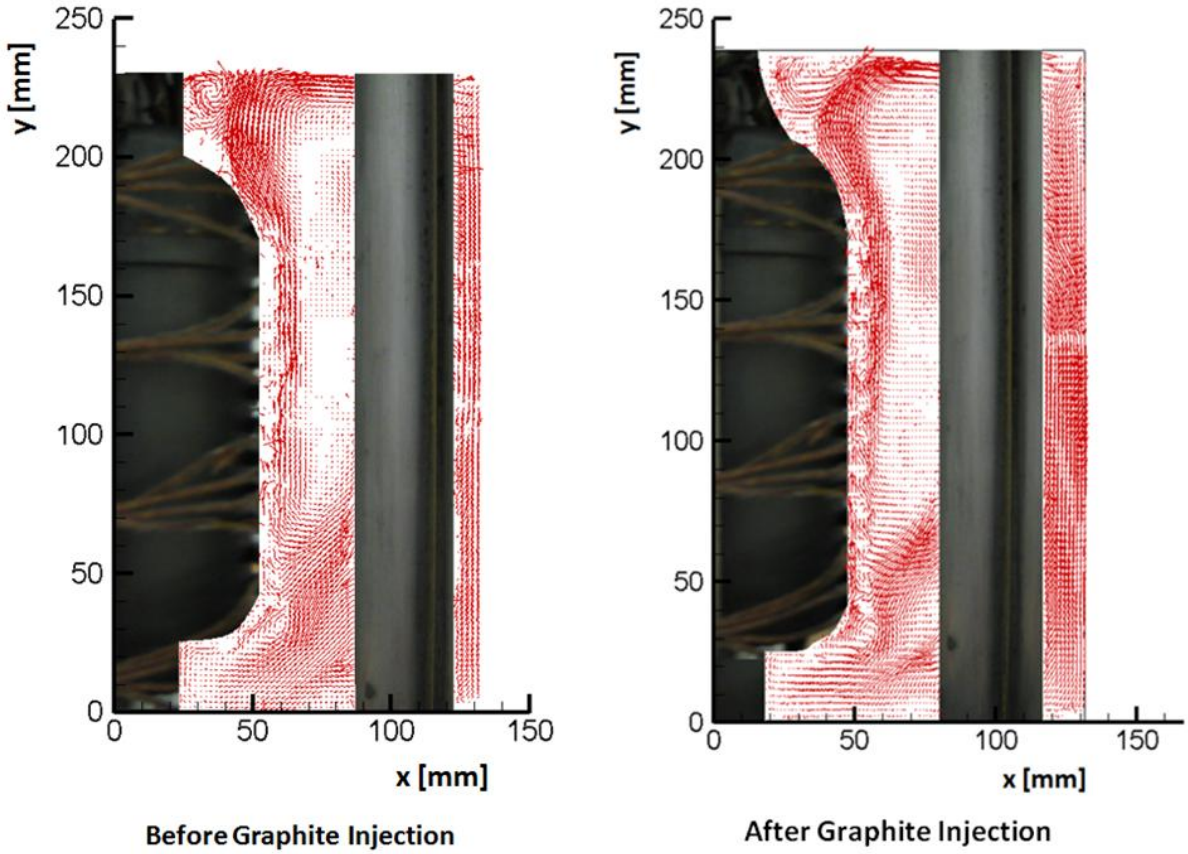

Figure 26. Air Velocity Field inside the Cavity

In both pictures, the main air recirculation cell is easily visible. The air flows upward near the surface of the vessel, due to the buoyancy forces induced by the lower density of the hot air near the vessel. At the top of the cavity the air hit the top plate and moves towards the back of the cavity passing through the risers. The relatively colder air

now flows downwards through the back cavity and starts again its path once reached the bottom. In the same picture two main vertices are also easily distinguishable. The vortex at the top, mainly induced by the upward air flow hitting the roof of the cavity, produces an “isolated” spot (Figure 26, top left of each picture), where the air is confined. The vortex near the bottom of the reactor vessel is produced by the combination of the air flow coming back cavity and the air rising from the bottom of the cavity. Air velocity pattern in the main cavity is characterized in both cases by relatively high magnitude, especially near the reactor vessel and change in direction due to the recirculation, while a regular velocity profile can be seen in the back cavity. The perturbations induced by the thermocouples places at the surface of the reactor vessel are clearly visible in Figure 26 as well as Figure 27.

No appreciable differences were observed in the air flow patterns inside the cavity before and after graphite dispersion. The comparison of the horizontal (u) and vertical (v) components of the velocity of the air inside the cavity before and after the graphite injection, shown in Figure 27, confirms this statement.

As mentioned in the previous section, the region at the top of the cavity is characterized by a large vortex which causes high velocity (see u-component in Figure 27). This effect, combined with the high temperature of the air at the top of the cavity, causes the hot spot in the top panel of the cavity already discussed.

As it can be observed qualitatively in Figure 26 and quantitatively in Figure 27 the air in the back cavity is characterized by a regular downward flow with low horizontal velocity component.

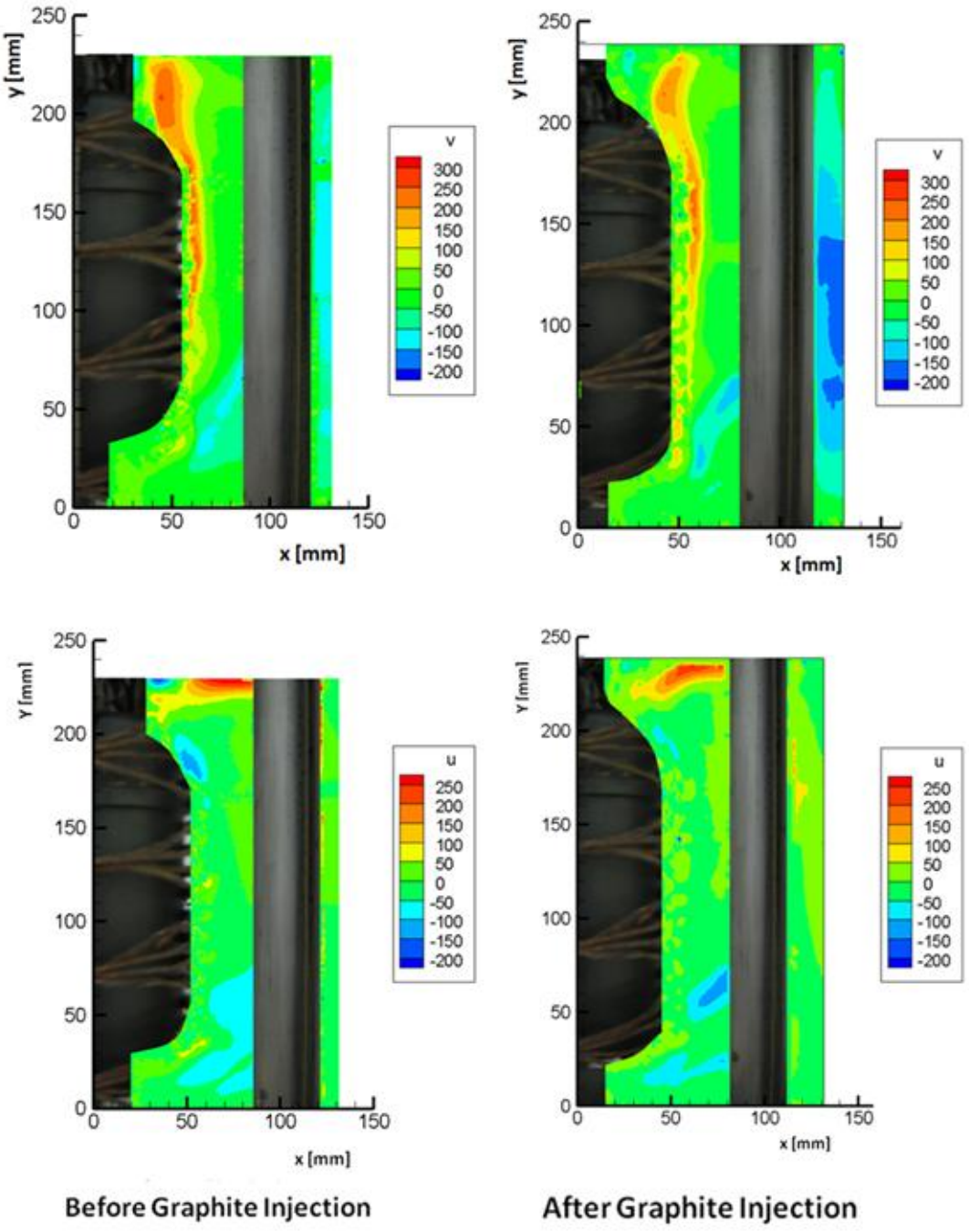

Figure 27. Horizontal (u) and Vertical (v) Components of the Velocity of Air

Standard errors for both u and v components, shown in Figure 28, were lower than 0.1 throughout the cavity except for peaks near the thermocouples locations on the vessel surface or at the top of the cavity.

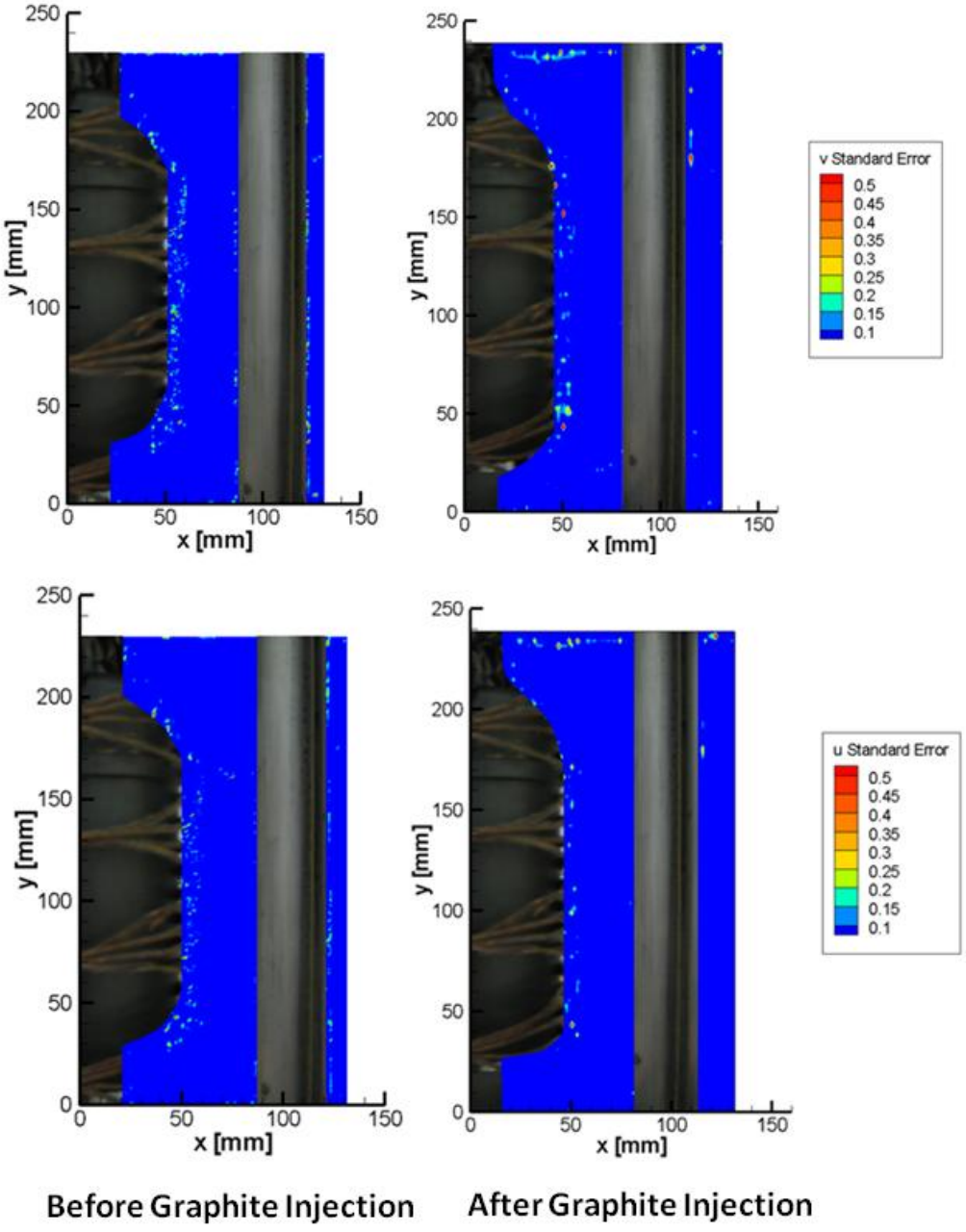

Figure 28. Air Velocity Components Standard Error

Most of the air flow pattern features inside the cavity were studied by direct observation of the air flow during the experiment thanks to the excellent illumination that was achieved with the PIV apparatus. Some of the most representative instantaneous pictures extracted from the movies recorded during the experiment with the high speed/resolution camera are reported in Appendix C

6. GRAPHITE EFFECT ANALYSIS

The effect of the graphite dispersion on the heat transfer mechanism in the reactor cavity was quantitatively analyzed by writing the energy balance in the cavity between under steady-state conditions. The total heat flux produced in the reactor vessel must be equal to the heat flux transferred by convection and the heat flux transferred by radiation to the pipes walls.

$$q''_{total} = q''_{convection} + q''_{radiation} \quad (1)$$

It must be remarked that heat losses through the cavity walls were neglected in Equation (1). The convection term $q''_{convection}$ can be expressed in terms of the convection heat transfer coefficient and the temperatures of vessel and pipes surfaces by the *Newton's law of cooling*. The radiation term $q''_{radiation}$ can be expressed in terms of the temperatures and emissivity of vessel and pipe surfaces and by the *Stefan-Boltzmann law*. Equation (1) can be re-written as follows:

$$q''_{total} = h(T_{vessel} - T_{pipes}) + \overline{F}_{vessel \to pipe}\sigma\left(T_{vessel}^4 - T_{pipes}^4\right) \quad (1a)$$

The observation and analysis of the air velocity using PIV described in the previous section allowed to consider negligible the change in the convective heat transfer coefficient induced by the graphite. Since the same total heat flux was imposed for both experiments with and without graphite, the change in the surface temperatures previously presented could be related as expected to a change in the emissivity of the

cavity surfaces and, subsequently, in the fraction of the total heat transferred by radiation.

Before Graphite Injection [b.g.]

$$q''_{tot} = \left[\overline{F}_{vessel \to pipe}\right]_{b.g.} \left(T^4_{vessel} - T^4_{pipes}\right)_{b.g.} + h\left(T_{vessel} - T_{pipes}\right)_{b.g.} \quad (2)$$

After Graphite Injection [a.g]

$$q''_{tot} = \left[\overline{F}_{vessel \to pipe}\right]_{a.g.} \left(T^4_{vessel} - T^4_{pipes}\right)_{a.g.} + h\left(T_{vessel} - T_{pipes}\right)_{a.g.} \quad (3)$$

The ratio of the view factors before and after graphite injection can be derived from Equations (2) and (3):

$$\frac{\Delta\left[\overline{F}_{vessel \to pipe}\right]}{\left[\overline{F}_{vessel \to pipe}\right]_{b.g.}} = \frac{\left(T^4_{vessel} - T^4_{pipes}\right)_{b.g.}}{\left(T^4_{vessel} - T^4_{pipes}\right)_{a.g.}} \left(1 - \frac{\left(T_{vessel} - T_{pipes}\right)_{a.g.}}{\left(T_{vessel} - T_{pipes}\right)_{b.g.}}\right) + 1 \quad (4)$$

Substituting the average temperatures before and after graphite dispersion summarized in Table II in Equation (4), the change in the view factor was found to be:

$$\frac{\Delta\left[\overline{F}_{vessel \to pipe}\right]}{\left[\overline{F}_{vessel \to pipe}\right]_{b.g.}} = +1.54\% \quad (5)$$

7. CONCLUSIONS

The effects of the graphite dispersion on the thermal hydraulic behavior Reactor Cavity Cooling System were empirically studied and analyzed using the RCCS experimental facility at the Department of Nuclear Engineering of Texas A&M University. Particle Image Velocimetry technique, direct flow visualization and temperature measures were applied during the experiment. The analysis of the velocity maps obtained with the PIV technique allowed to qualitatively analyze the natural circulation of the air inside the reactor cavity and showed enhanced vortices near the top and the bottom heads of the vessel. The comparison of the results obtained before and after the graphite dispersion did not find appreciable differences in the velocity components magnitude or flow patterns allowing neglecting the variation of the convective heat transfer coefficient induced by the graphite. In both cases low velocity magnitude and regular parallel streamlines were observed in the back cavity of the experimental facility. The temperature profiles of the reactor vessel and standing pipes were observed to change when graphite was dispersed into the cavity. The energy balance equation for the cavity was used to calculate the change in the radiant view factor of the cavity induced by the graphite particles deposition, under the assumptions of negligible heat losses through the thermically insulated cavity walls. The increase of the cavity view factor was estimated to be as high as 1.54%. This increase can be directly related to the change in the emissivity of the surfaces produced by the graphite deposition. The results obtained during this experimental activity give an important

contribution in the understanding of the thermal hydraulic behavior of the reactor cavity cooling system, confirming its potentiality as passive heat removal system also during accident scenarios such as the Depressurized Conduction Cooling event, which was considered as one of the most demanding accidents that have to be analyzed for the next generation nuclear reactors.

8. FUTURE WORK

The Department of Nuclear Engineering of Texas A&M University will host a new experimental facility to continue to experimental study of the thermal hydraulic phenomena in the Reactor Cavity Cooling System of a VHTR, as part of the same project sponsored by the US Department Of Energy (DOE) and the Nuclear Energy University Program (NEUP). The model will be a small scale (1/16) of the full scale cooling system representing a portion of the reactor vessel and one cooling panel with 9 stainless steel risers. In the first stage of the research project, water will be used as coolant to study the phenomena involving the natural circulation of the water during accident scenario. The facility will reproduce the cavity and was designed to perform temperature measurements in the cavity and risers walls, heat flux measurements in the riser's walls and flow visualization inside the risers, at the top and bottom manifolds and in the water tank. The total power installed in the facility will be approximately 24kW. The experimental results will be available during 2011.

REFERENCES

Capone, L., Estrada Perez, C.E., Hassan, Y.A., 2010a. Experimental investigation of a Reactor Cavity Cooling System for a Very High Temperature Reactor.18th International Conference of Nuclear Engineering ICONE 18 Xi'an China.

Capone, L., Vaghetto, R., Hassan, Y., 2010b. Graphite Dispersion Effects experimental Analysis for a Reactor Cavity Cooling System (RCCS). American Nuclear Society 2010 Winter Meeting November 7-11 Las Vegas Nevada.

Estrada-Perez, C.E., Hassan, Y.A., 2010. PTV experiments of subcooled boiling flow through a vertical rectangular channel, International Journal of Multiphase Flow 36 (2010) 691–706.

Hassan, Y.A., Blanchat, T.K., Seeley Jr., C.H., Canaan, R.E., 1992. Simultaneous velocity measurements of both components of two phase flow using particle image velocimetry, Int. J. Multiphase Flow 18 (1992) 371–395.

Kissane, M.P., Zhange, F., Reeks, M.W., 2010. Dust in HTRs: its Nature and Improving Prediction of its Resuspension. Proceedings of HTR 2010, Prague, Czech Republic, October 18-20 2010 Paper 219.

Loyalka, S.K., 1983. Mechanics of Aerosols In Nuclear Reactor Safety: A Review. Progress in Nuclear Energy, (1983) Vol. 12, No. 1, pp. 1-56.

Van Antwerpen, H.J., Greyvenstein, G.P., 2008. Evaluation of a detailed radiation heat transfer model in a high temperature reactor systems simulation model. Nuclear Engineering and Design 238 (2008) 2985–2994.

Supplemental Sources Consulted

Adrian, R.J., 1991. Particle-imaging techniques for experimental fluid mechanics, Annual Rev. Fluid Mech. 23 (1991) 261–304.

Ali, M., 2009. Natural convection heat transfer along vertical rectangular ducts. Heat Mass Transfer (2009) 46:255–266.

Farmer, M.T., Kilsdonk, D.J., Tzanos, C.P., Lomperski, S., Aeschlimann, R.W., Pointer, D., 2009. Natural Convection Shutdown Heat Removal Test Facility (NSTF) Evaluation for Generating Additional Reactor Cavity Cooling System (RCCS) Data. ANL-GenIV-058.

Loyalka, S.K., 1983. Mechanics of Aerosols In Nuclear Reactor Safety: A Review. Progress in Nuclear Energy, (1983) Vol. 12, No. 1, pp. 1-56.

Thielman, J., Ge, P., Wu, Q., Parme, L., 2005. Evaluation and Optimization of General Atomic's GT-MHR reactor cavity cooling system using an axiomatic design approach. Nuclear Engineering and Design 235(2005) 1389-1402.

Tzanos, C.P., Farmer, M.T., 2009. Feasibility Study of the Natural Convection Shutdown Heat Removal Test Facility (NSTF) for Initial VHTR Water-Cooled RCCS Shutdown. ANL-GenIV-079.

Verwey, Dobson, R.T., 2010. Modeling and Optimization of a Reactor Cavity Cooling System (RCCS) subject to changes in Ambient Conditions. Proceedings of HTR 2010, Prague, Czech Republic, October 18-20 2010.

APPENDIX A – ADDITIONAL PICTURES OF THE EXPERIMENTAL FACILITY

A set of extra pictures were collected during the experiment and are presented in this Appendix to give additional to the reader additional details of the experimental facility and its instrumentation.

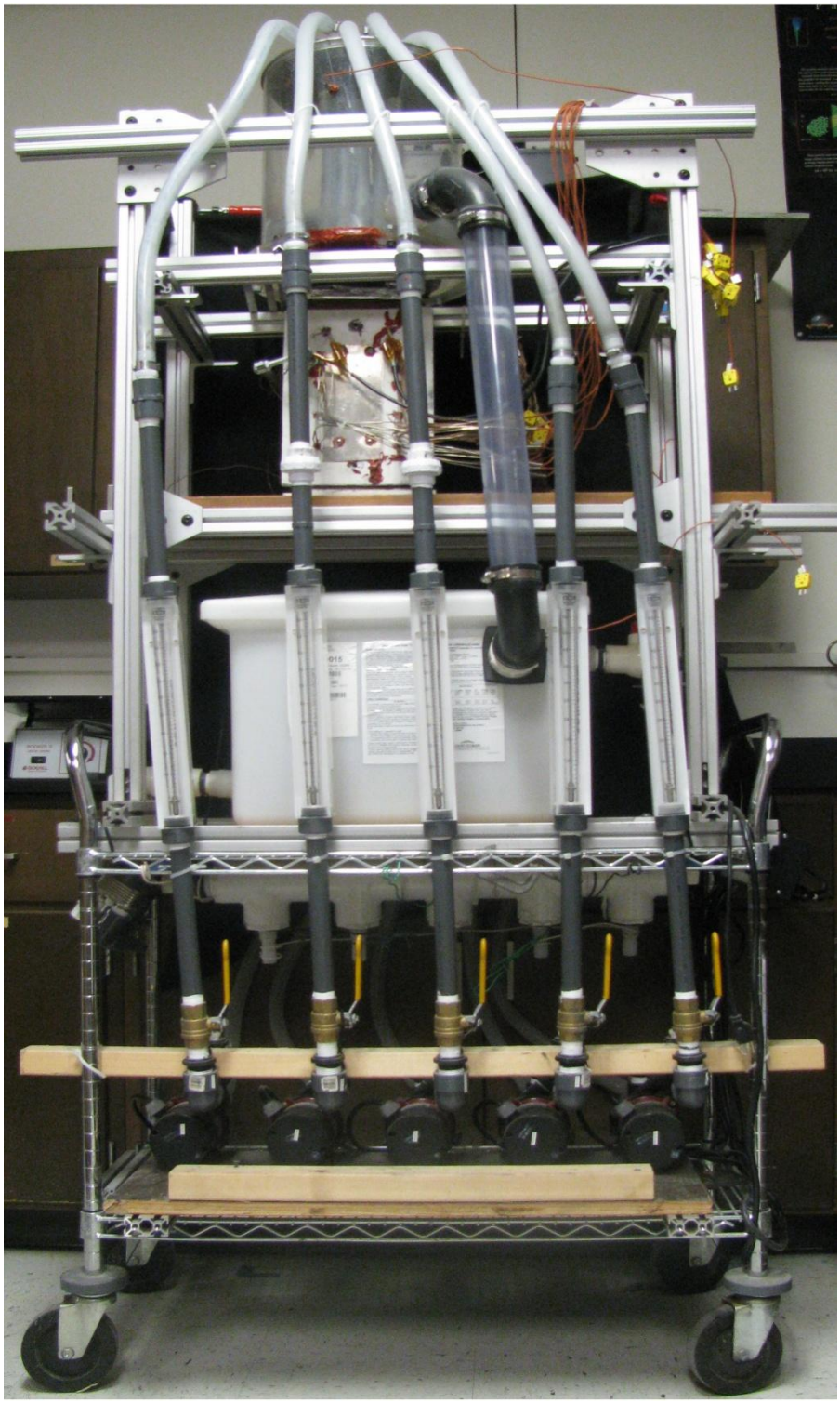

Figure A 1. Experimental Facility (Back View)

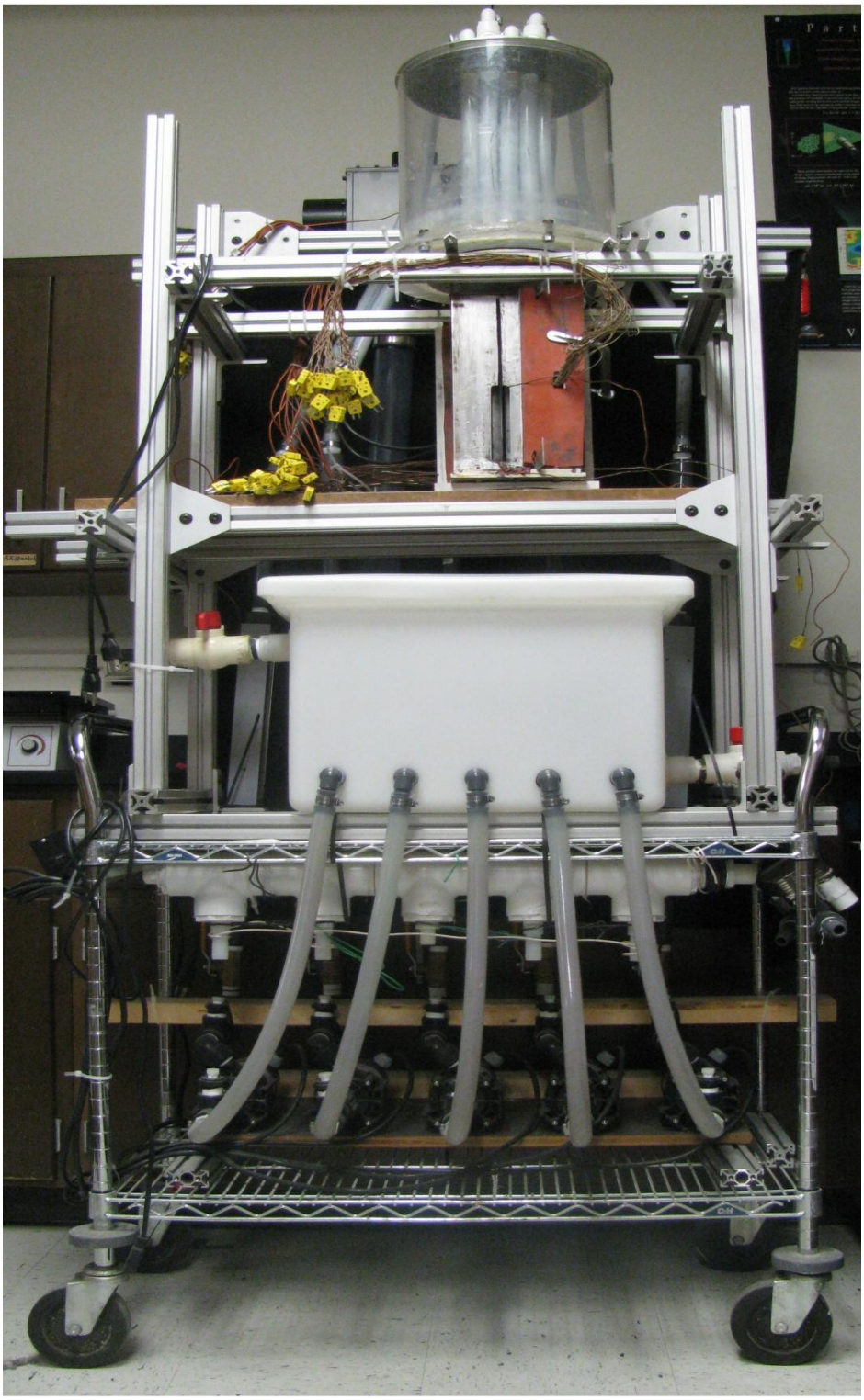

Figure A 2. Experimental Facility (Front View)

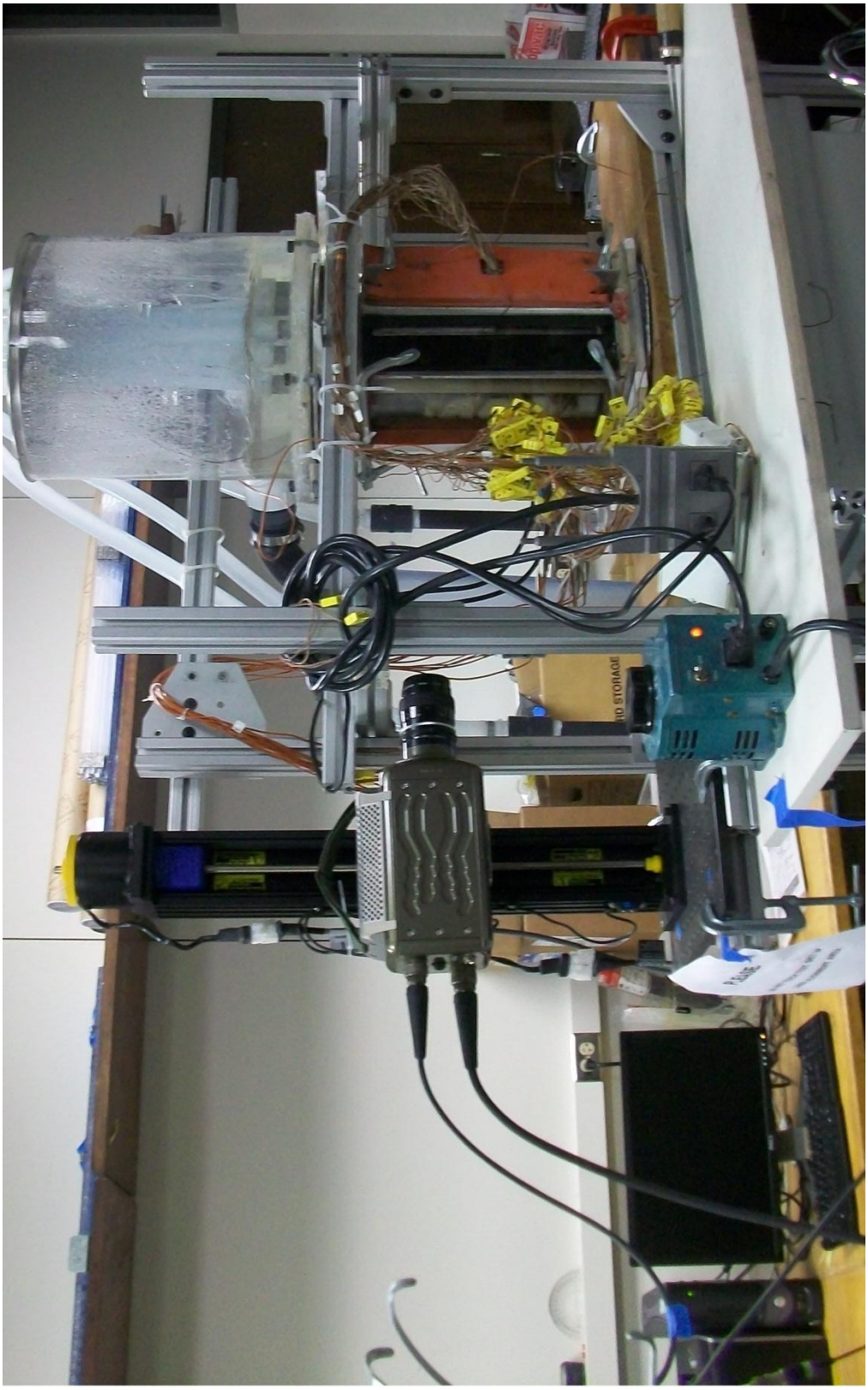

Figure A 3. Visualization Apparatus

Figure A 4. Vessel (Before Graphite Dispersion)

\

Figure A 5. Vessel (Before Graphite Dispersion)

APPENDIX B – AIR TEMPERATURE PROFILES INSIDE THE CAVITY

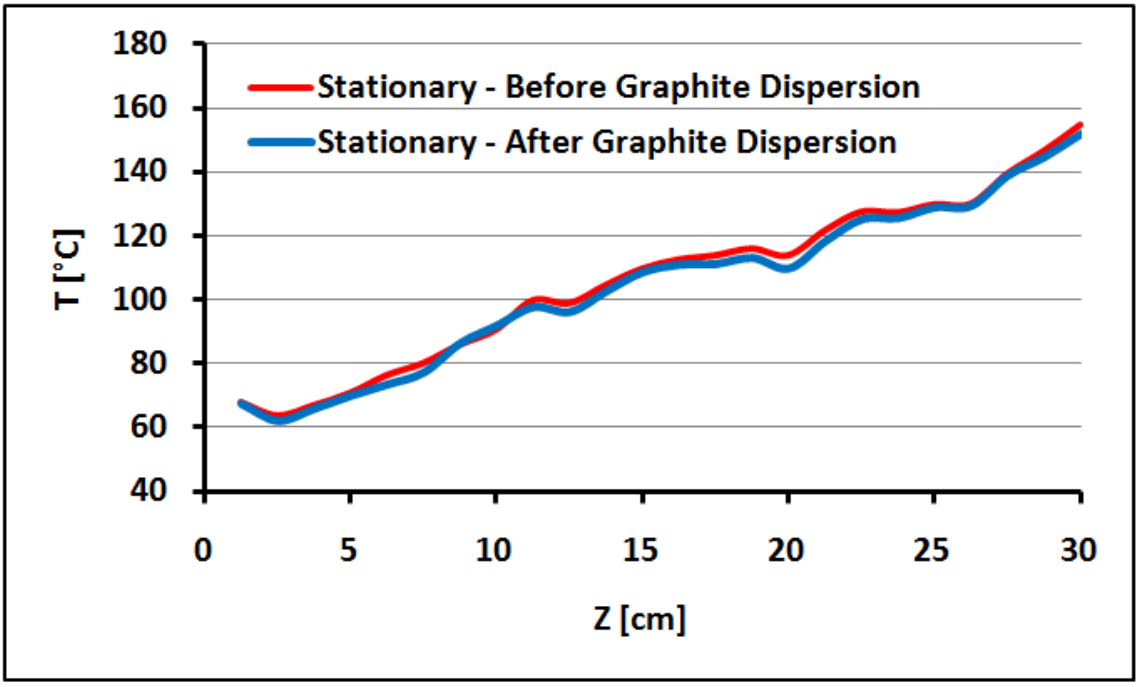

Figure B 1. Air Temperature profile (Middle of the Cavity)

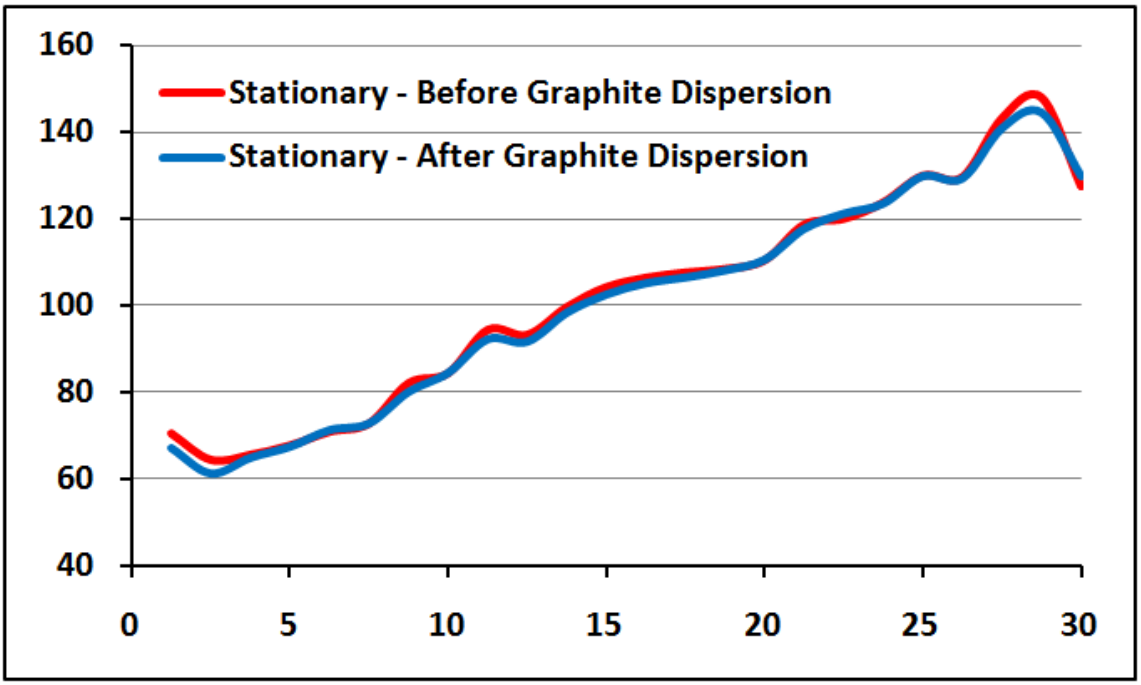

Figure B 2. Air Temperature profile (Far from the Vessel)

APPENDIX C – AIR FLOW VISUALIZATION (SNAPSHOTS)

Figure C 1. Air Flow Visualization (Top Region)

Figure C 2. Air Flow Visualization (Middle-Top Region)

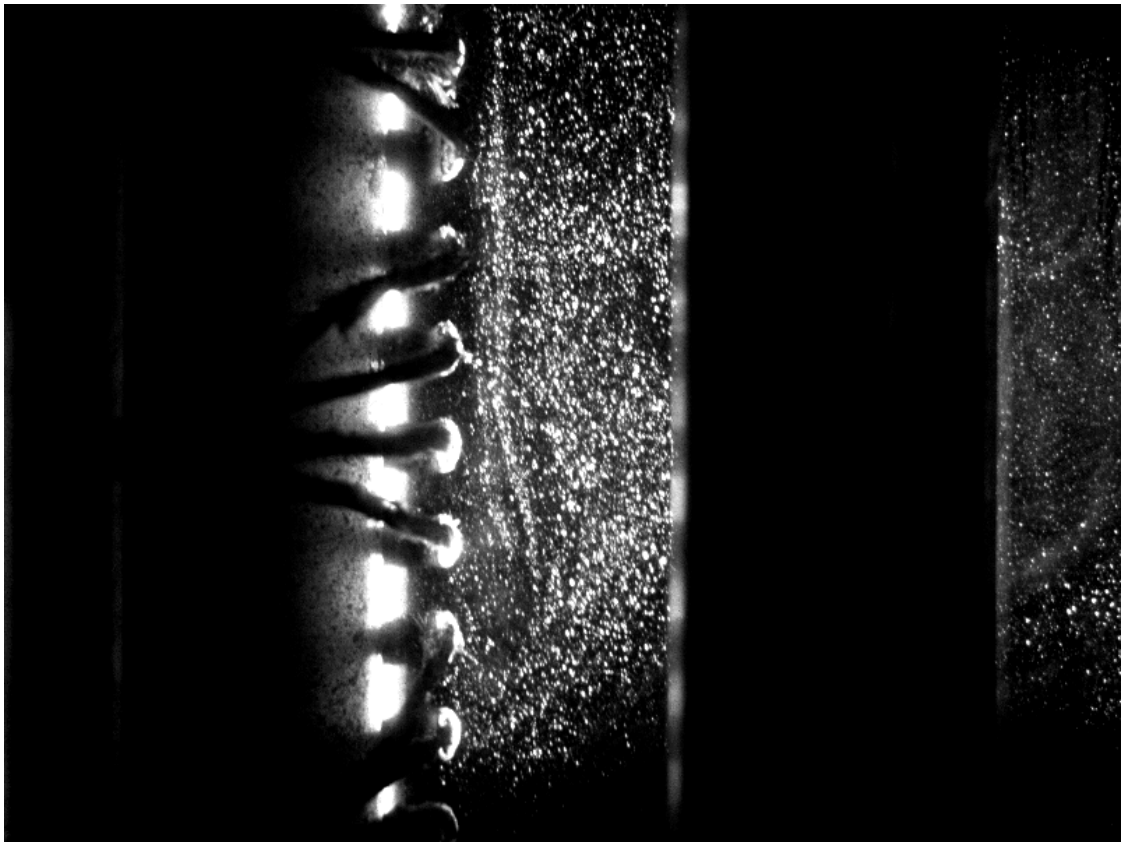

Figure C 3. Air Flow Visualization (Middle-Bottom Region)

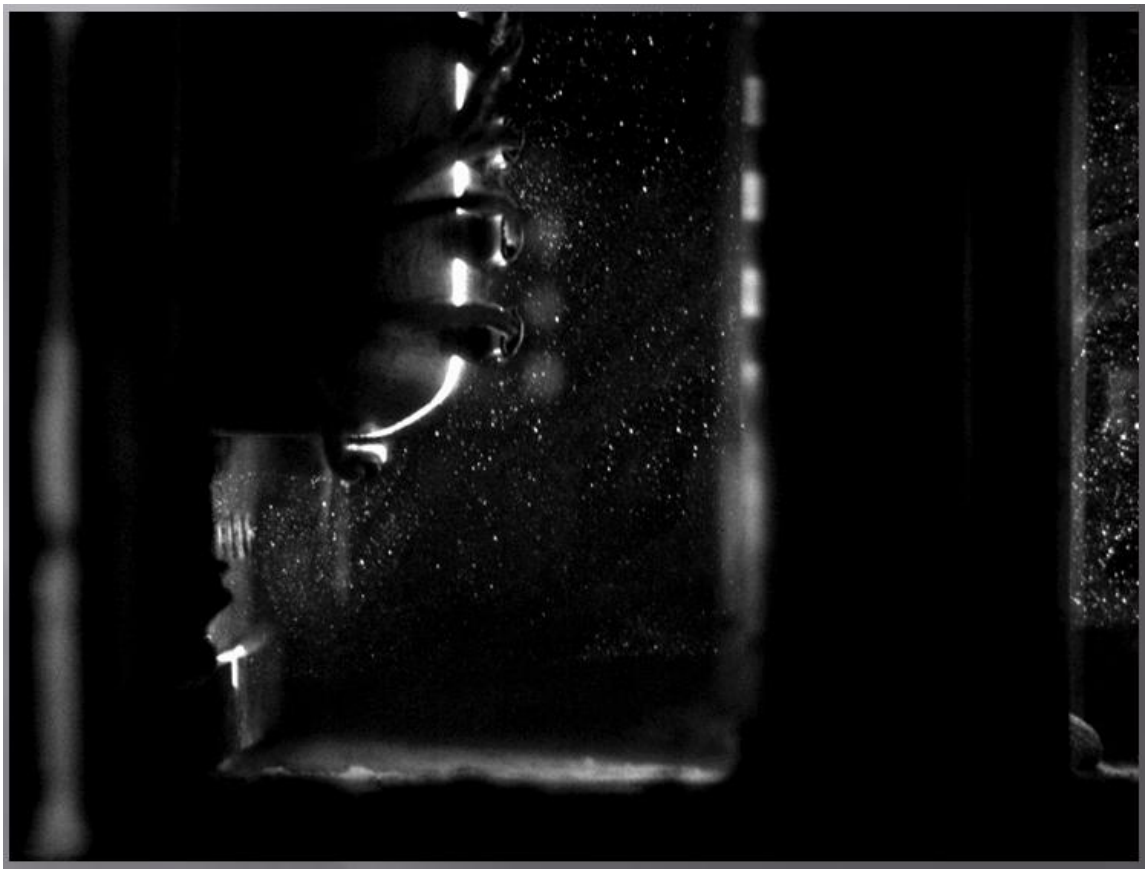

Figure C 4. Air Flow Visualization (Bottom Region)

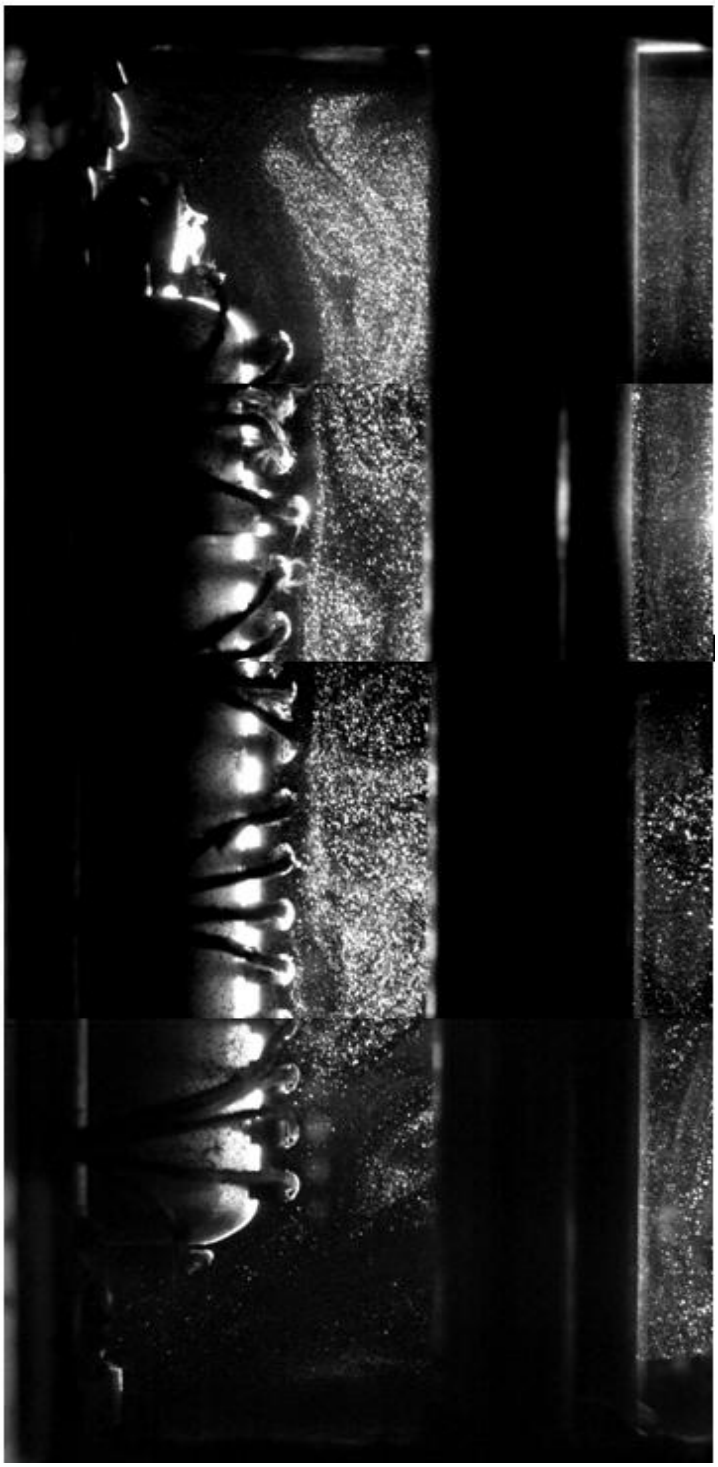

Figure C 5. Air Flow Visualization (Full Cavity)

VITA

Rodolfo Vaghetto was born in Palermo, Italy. He obtained his B.En. degree in nuclear engineering at the University of Palermo in April 2000. He worked at the Department of Nuclear Engineering of the same university as a researcher, focusing his attention and interest on the analysis of thermal-hydraulic phenomena in Light Water Reactors and Accelerator Driven Systems (ADS) using RELAP5. In April 2001 he joined STMicroelectronics and started his career as product engineer and project manager. After eight years of experience in the same company he decided to pursue his interest in the nuclear power generation. He received his M.S. degree in nuclear engineering from Texas A&M University in May 2011. He is currently enrolled in the Ph.D. program. His current projects involve experimental studies of the Reactor Cavity Cooling System of the new generation nuclear power plants and computational analysis of the same systems using RELAP5-3D. He may be reached at the Department of Nuclear Engineering of Texas A&M University, 3133 TAMU, College Station, TX 77843-3133.